

## The Heavy Nuclei of the Primary Cosmic Radiation

H. L. BRADT AND B. PETERS  
*University of Rochester, Rochester, New York*  
 (Received September 9, 1949)

The flux of primary cosmic-ray nuclei, heavier than protons, was determined at geomagnetic latitudes  $\lambda=55^\circ$  and  $\lambda=30^\circ$ N. It is shown that at  $\lambda=30^\circ$  at least one-half of the incident nucleons and a significant fraction of the incident cosmic-ray energy is due to the heavy component.

The distribution of atomic numbers among the primaries was determined at both latitudes; the relative magnitude of the fluxes of the nuclei H:He:C,N,O:(nuclei of charge  $Z>10$ ) is given approximately by the ratio 4000:1000:35:10.

The possible significance of these results for the theories on the origin of cosmic rays is discussed.

IN previous papers<sup>1-3</sup> evidence has been presented for the occurrence of heavy nuclei in the primary cosmic radiation. Methods have been discussed for determining the charge of these nuclei from the analysis of the tracks they produce when traversing nuclear emulsions.

In this paper we shall present more extensive data on the flux, charge spectrum, and energy distribution of the primary cosmic rays of charge  $Z>1$ .

The discussion is divided into the following topics:

- Section I. Evidence for the primary character of energetic heavy nuclei.
- Section II. The identification of particles and the flux of primary helium nuclei.
- Section III. The mean free path for nuclear collisions of heavy cosmic-ray primaries.
- Section IV. The flux of primary cosmic rays of charge  $Z\geq 6$ .
- Section V. The low energy part of the spectrum at  $\lambda=55^\circ$ .
- Section VI. The contribution of heavy primary nuclei to the total primary and secondary radiation.
- Section VII. The latitude effect of the heavy primary radiation and its energy spectrum.
- Section VIII. The relative abundance of the different elements in the primary radiation.
- Section IX. Remarks on the origin of cosmic radiation.

Our investigations are based on the tracks of particles in emulsions of large stacks of photographic plates<sup>2</sup> exposed at altitudes corresponding to about 16 g/cm<sup>2</sup> of residual atmosphere.

The results presented in this paper are mainly de-

rived from four high altitude balloon flights, for which the relevant data are listed below in Table I.

### I. EVIDENCE FOR THE PRIMARY CHARACTER OF ENERGETIC HEAVY NUCLEI

Our original conclusion that the energetic heavy nuclei observed at high altitudes are cosmic-ray primaries has been greatly strengthened by later observations and it therefore seems desirable to summarize the present evidence.

#### A

Several hundred particles with at least several g/cm<sup>2</sup> residual range and atomic number  $Z\geq 6$  were recorded in a systematic survey; none has been found to originate in the stack of plates of dimensions 50-100 g/cm<sup>2</sup> exposed below 16 g/cm<sup>2</sup> of residual air unless it was the disintegration product of a still heavier incident nucleus. Thus, if the energetic heavy nuclei are secondaries, they could only be produced by a particle which is destroyed at the very top of the atmosphere with a mean free path for destruction of only a few g/cm<sup>2</sup>. The collision cross section of such a particle would therefore have to be extremely large.

Heavy fragments with charges up to  $Z\sim 10$  are occasionally emitted in violent nuclear explosions produced by neutral or singly charged particles, but their ranges rarely exceed a few hundred microns.<sup>4</sup>

TABLE I.

Flight No.	Date	Geographical location lat. long.	Geomagn. latitude	Material above plates (mainly air) (in g/cm <sup>2</sup> )	Time of exposure (hours)	Size of stack
1	10-27-48	44°N 94°W	55°N	16	5	58 plates (3 in.×20 in.)
2	2-4-49	19°N 79°W	30°N	16	6	25 plates (3 in.×10 in.)
3	5-29-49	40°N 76°W	51°N	~10	3	24 plates (3 in.×10 in.)
4	7-30-49	44°N 94°W	55°N	16	6	24 plates (1 in.×3 in.)

<sup>1</sup> Freier, Lofgren, Ney, Oppenheimer, Bradt, and Peters, Phys. Rev. **74**, 213 (1948).

<sup>2</sup> H. L. Bradt and B. Peters, Phys. Rev. **74**, 1828 (1948).

<sup>3</sup> Freier, Lofgren, Ney, and Oppenheimer, Phys. Rev. **74**, 1818 (1948).

<sup>4</sup> A. Bonnetti and C. Dillworth, Phil. Mag. **40**, 585 (1949).

## B

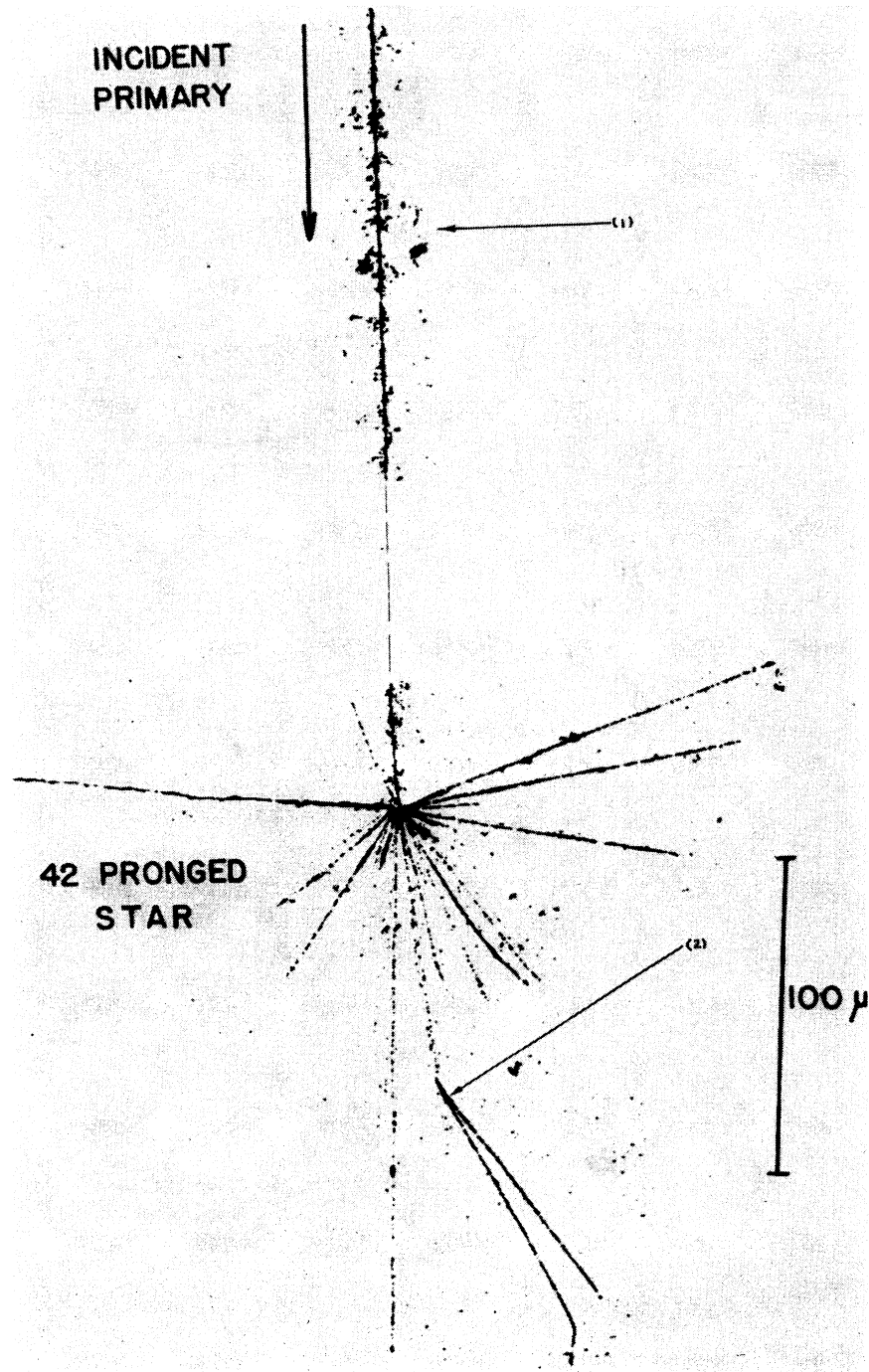
All observations indicate that the energetic heavy particles enter from the upper hemisphere. The direction of motion of the particle is known:

(1) If the particle slows down as evidenced by a rapid increase in  $\delta$ -ray density (approximately fifty such cases have been observed, all of which show downward motion).

(2) If one end of the track terminates in a nuclear explosion in the photographic emulsion (Fig. 1). It should be the lower end of the track if the particle produced the star and the upper end if it originated in the star. (In all cases observed, with the exception of tracks of fragments of still heavier nuclei, it is the lower end of the track which terminates in a star.)

(3) If the particle undergoes a nuclear collision in the glass in which it is only partially destroyed.<sup>5</sup> The particle then emerges

FIG. 1. Collision of a primary Ca nucleus ( $Z=20\pm 1$ ) with an energy of the order of at least 100 Bev and an Ag or Br nucleus of a Kodak NTB3 emulsion, flown in Flight No. 2 at  $\lambda=30^\circ\text{N}$ . 42 charged particles are emitted in this violent explosion. 10 prongs are minimum ionization tracks, collimated in the forward direction (they are hardly visible in Fig. 1); most of them probably are tracks of a meson shower. One fast, singly charged particle causes a second nuclear event (2).



<sup>5</sup> H. L. Bradt and B. Peters, Phys. Rev. 75, 1779 (1949).

with reduced charge accompanied by satellites consisting of fast protons and  $\alpha$ -particles (see Fig. 3 of reference 5). (About 40 such cases have been observed, all of which show downward motion.)

C

There is an observable concentration of heavy tracks around the zenith direction in plates exposed below

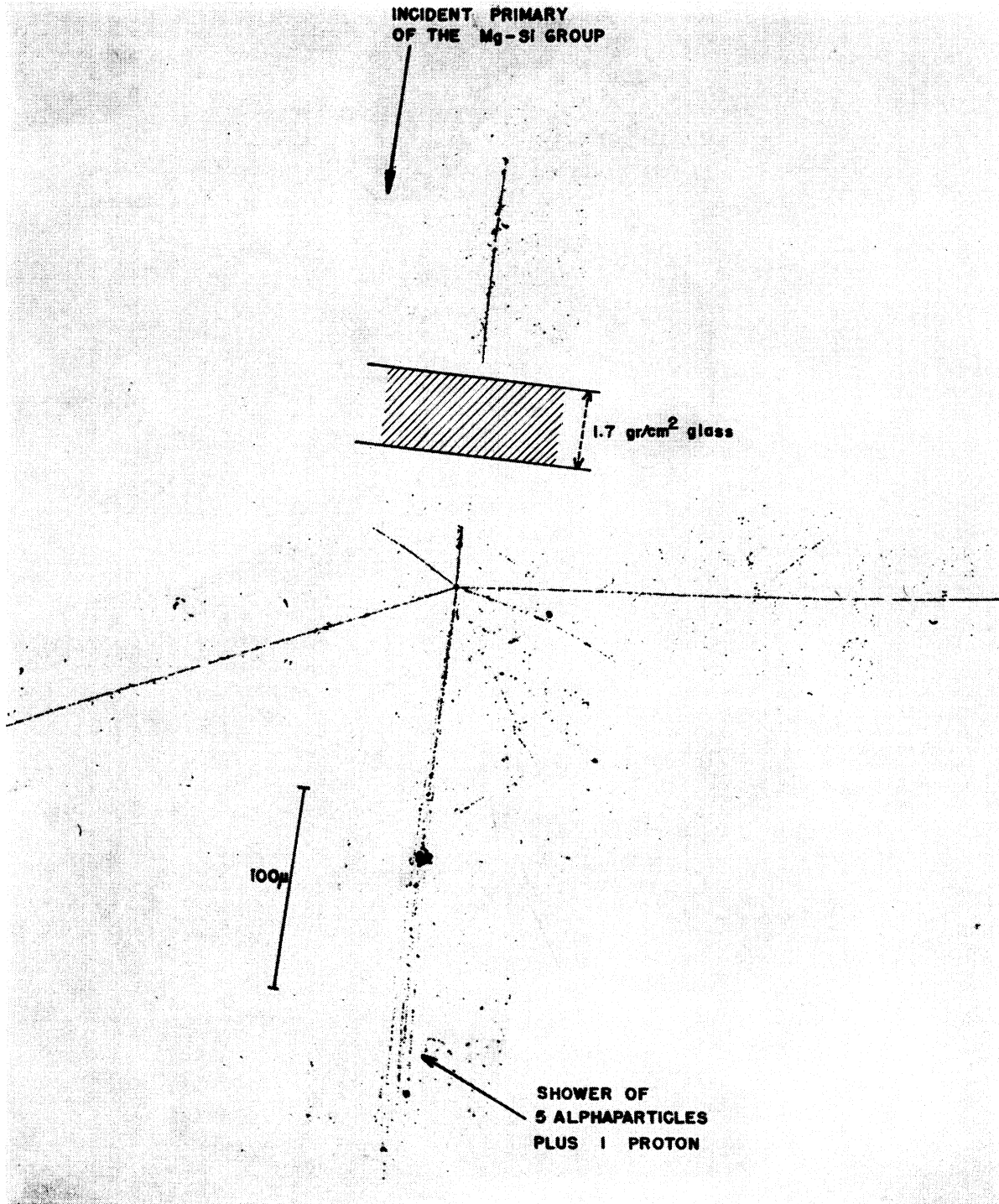


FIG. 2a. Collision of a nucleus of the Mg-Si group ( $Z \sim 12-14$ ), resulting in a narrow shower of five doubly charged relativistic particles ( $\alpha$ -particles) and one singly charged relativistic particle (proton). The particles of the shower, carrying 11 units of charge, are considered to be the products of the dissociation of the incident nucleus. A second minimum ionization track emerges with an angle of  $30^\circ$  with respect to the shower axis. Four low energy particles ejected from the star at large angles with respect to the direction of the primary are considered to be fragments of the target nucleus.

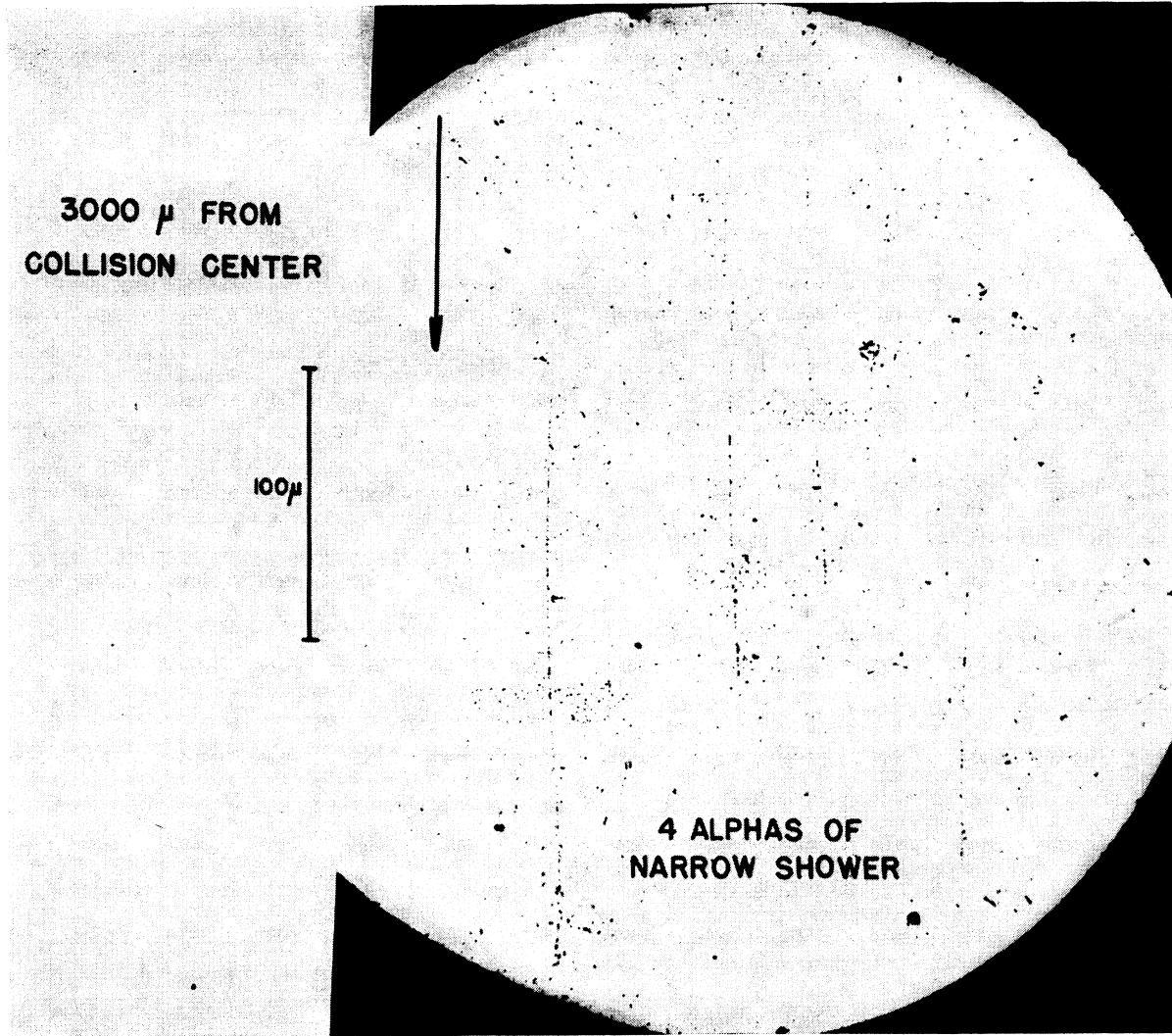


FIG. 2b. Tracks of 4 of the 5 alpha-particles of the shower of Fig. 2a as they appear in the next plate of the stack, after traversal of 3-mm glass. The average angle of the tracks of the five alpha-particles with respect to the axis of the shower is 0.03 radian, corresponding to an energy of the incident nucleus of  $\sim(3-4)$  Bev per nucleon.

16 g/cm<sup>2</sup> of air. This indicates a flux of particles entering from the upper hemisphere with an absorption mean free path of the order of, but longer than, 16 g/cm<sup>2</sup> of air. In a previous communication<sup>5</sup> we have reported values for the mean free path obtained from direct measurements and have shown that these values are consistent with the size of the nuclei as obtained from our charge determination.

#### D

It has been established with certainty that some of the nuclei observed have atomic numbers much greater than that of air nuclei. This has been demonstrated previously<sup>2</sup> by the self-consistency of charge determinations obtained from  $\delta$ -ray densities over wide ranges of residual path lengths. It is also conclusively demonstrated by collisions of the type illustrated in

Fig. 2, as will be discussed later. Nuclei which are heavier than air nuclei obviously must arrive from the outside.

While the facts listed above show, in our opinion, conclusively that the heavy nuclei observed are not created by a primary proton component, they, of course, do not rule out the possibility that these nuclei may arrive as part of still larger structures.

A plausible mechanism whereby dust grains could be accelerated by the radiation pressure in the neighborhood of supernovae up to energies of the order of 1 Bev per nucleon has recently been suggested by Spitzer.<sup>6</sup> We therefore shall consider the possibility that the heavy primaries observed are remains of larger structures such as dust grains, although energies of the

<sup>6</sup> L. Spitzer, Phys. Rev. **76**, 583 (1949).

TABLE II.  $\delta$ -ray count for the track of an iron atom (Flight No. 1),  $Z=26\pm 2$ 

Plate	Residual range $R(\text{gr}/\text{cm}^2)$	$\beta = v/c$	$\delta$ -rays/100 $\mu$ observed	$Z=24$	$Z=26$	$Z=28$
				$\delta$ -rays/ 100 $\mu$	calcu- lated	
321	26.0	0.85	$26\pm 4$	24	28	32
361	21.6	0.83	$32\pm 4$	26	30	35
401	16.4	0.80	$35\pm 4$	27	32	37
451	10.0	0.73	$39\pm 4$	32	38	44

heavy nuclei at least as high as 10 Bev/nucleon have been observed.<sup>5</sup> In discussing Spitzer's hypothesis, the following alternatives must be considered separately:

(1) The heavy nuclei observed may be the product of the break-up of fast dust grains due to collisions *in interstellar space*. Our observations certainly admit this possibility.

(2) An appreciable number of such dust particles may not break up in interstellar space but succeed in penetrating the earth's magnetic field and break up into atoms only *at the top of the atmosphere*.

On the basis of (2) we must expect:

(a) The appearance of large narrow-angle showers of heavy nuclei. There is as yet no evidence for the existence of such showers.

(b) The absence of a latitude effect. The ratio charge/mass  $=Z/M$  must be exceedingly small for any dust particle and therefore its trajectory must be insensitive to the earth's magnetic field. However, even with assumption (2) we may expect a mixture of dust particles and its disintegration products entering the earth's magnetic field. In that case the latitude effect will depend among other things, on whether the atomic products of the disintegrated dust have been completely stripped of electrons before entering the earth field. It seems unlikely that heavy ions should be completely stripped of electrons in passage through a given amount of matter while the same amount of matter is incapable of disintegrating dust particles of the same velocity into atoms, but this point may require closer study.

(c) The mechanism suggested by Spitzer requires that in addition to very high energy dust particles, a much larger number of dust particles with lower energy should be produced. Therefore even if only a small fraction of undisintegrated dust penetrated the earth's magnetic field at latitude  $\lambda=30^\circ$  we should nevertheless observe even at this latitude heavy nuclei of low energy.

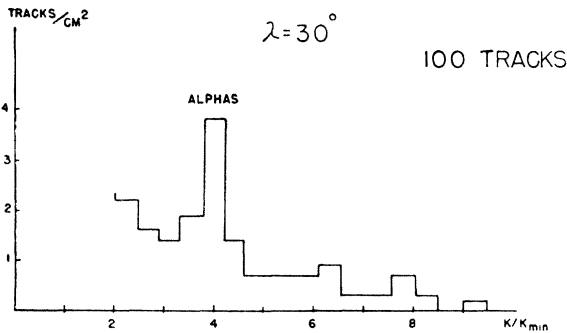


FIG. 3. Frequency of 100 tracks of length  $L \geq 750\mu$  in an area of  $5.8 \text{ cm}^2$  emulsion of plate No. 190 flown at  $\lambda=30^\circ$  plotted against the specific energy loss  $K$  (in units of the minimum energy loss of singly charged particles  $K_{\text{min}}$ ) corresponding to their grain density. A definite peak occurs for  $K=4K_{\text{min}}$ ; this peak is ascribed to primary  $\alpha$ -particles.

TABLE III. Observed and calculated specific energy loss for a fast carbon nucleus.

	Residual range $R=13.7 \text{ g}/\text{cm}^2$				Residual range $R=6.8 \text{ g}/\text{cm}^2$			
	$Z$	$K$	$v/c$	$n_\delta$	$K$	$v/c$	$n_\delta$	
observed		120-140		$1.9\pm 2$	140-160		$2.9\pm 2$	
calculated	6	120	0.59	2.0	160	0.51	2.8	
	7	155	0.61	2.6	205	0.53	3.7	
	8	190	0.63	3.3	250	0.55	4.8	

Among some 200 tracks of heavy nuclei observed so far at  $\lambda=30^\circ$  we have found none which come to rest by ionization energy loss or show any increase in  $\delta$ -ray density due to a decrease in velocity; the particles either penetrate the stack or are destroyed by nuclear collisions. Thus at that latitude practically all particles must have energies of at least several Bev per nucleon.

It seems to us that the absence of low energy heavy nuclei at  $\lambda=30^\circ$  geomagnetic latitude is a strong argument against assumption (2). Thus, if heavy nuclei have originally been accelerated as dust grains, these grains must have been disintegrated *before* entering the region of the earth's magnetic field.

## II. THE IDENTIFICATION OF PARTICLES AND THE FLUX OF PRIMARY HELIUM NUCLEI

### A. Particles of charge $Z \geq 6$

The method used for obtaining, by  $\delta$ -ray count, the charge and mass of such particles has previously been discussed in detail.<sup>2</sup> Collisions like the one illustrated in Fig. 2, where a nucleus of charge  $Z=13\pm 1$  as determined from  $\delta$ -ray count gives rise to a very narrow shower consisting of one singly charged particle and five relativistic  $\alpha$ -particles (identified by grain count) furnish an independent check that the charge of the incoming nucleus was not overestimated appreciably by the method of  $\delta$ -ray counting. On the other hand, the fact that the highest  $Z$ -values we have found so far are, within an uncertainty of not more than two units, equal to  $Z=26$ , the atomic number of the heaviest element with appreciable cosmic abundance (iron), indicates that the charges of the heavy nuclei are also not underestimated.

In emulsions of high sensitivity, which show a comparatively large number of low energy electron tracks, the "background" of unrelated  $\delta$ -rays, which has to be subtracted from the observed number of  $\delta$ -rays, is not negligible for the lightest tracks. The background has been determined by comparing  $\delta$ -ray densities of long ( $\sim 25000\mu$ ) tracks of relativistic  $\alpha$ -particles with  $\delta$ -ray densities of minimum ionization tracks. In the plates flown at  $\lambda=30^\circ$  in Flight No. 2, for instance, the  $\delta$ -ray density for minimum ionization tracks was determined to  $n_1' = 0.26(\delta\text{-rays}/100)$ , the  $\delta$ -ray density of relativistic  $\alpha$ -particles to  $n_2' = 0.44(\delta\text{-rays}/100\mu)$ . Since the true  $\delta$ -ray density of relativistic  $\alpha$ -particles, corrected for background,  $n_2$ , must be four times greater than the corrected  $\delta$ -ray density of minimum ionization tracks  $n_1$ , we obtain for the  $\delta$ -ray calibration of these plates

$$(n_\delta)_Z = (0.060 \cdot Z^2 + 0.2)(\delta\text{-rays}/100\mu),$$

for particles of charge  $Z$  and  $\beta = v/c = 1$ .

For carbon and iron nuclei, this relation yields the values  $(n_\delta)_C = 2.4$  and  $(n_\delta)_{Fe} = 41$  ( $\delta$ -rays/100 $\mu$ ), respectively. The diagram of Fig. 10, which shows the frequency of tracks observed in these plates plotted against their  $\delta$ -ray density, shows a definite peak for  $n_\delta = (2.3 \pm 0.2)$  ( $\delta$ -rays/100 $\mu$ ), which is therefore ascribed to carbon nuclei. The highest  $\delta$ -ray densities observed are  $n_\delta \sim (39-45)$  ( $\delta$ -rays/100 $\mu$ ), therefore corresponding to charges close to the charge of an iron nucleus.

The same results were obtained in the other flights (see Fig. 11 and Fig. 12). The plates flown at  $\lambda = 55^\circ$  N in Flight No. 1, for instance, were somewhat less sensitive than the plates of Flight No. 2 and therefore less restrictive criteria were used for the  $\delta$ -ray counting. As an example, we present in Table II the results of the  $\delta$ -ray analysis of one of the heaviest tracks found in the plates of Flight No. 1, a photo-micrograph of which has been reproduced in Fig. 1 of reference 14. The calculated  $\delta$ -ray densities are based on a calibration corresponding to  $n_\delta \cdot \beta^2 = (1.1 \pm 0.1)$  ( $\delta$ -rays/100 $\mu$ ) for carbon nuclei.

We estimate the accuracy of our best charge determinations by  $\delta$ -ray count to be approximately  $\pm 10$  percent. However it is possible to improve the accuracy for nuclei of charge  $Z \lesssim 10$  by using plates sufficiently underdeveloped to permit grain counting. The accuracy obtainable by this method may be judged from the following example. Consider the track of a heavy particle which entered a stack of Ilford C2 plates making an angle  $\vartheta = 17^\circ$  with the zenith direction, traversed 6 plates (13.7 g/cm<sup>2</sup> of glass) and came to rest in the emulsion of the seventh plate. The sensitivity of the emulsion was calibrated by measuring the grain density of proton and meson tracks of varying residual ranges and plotting the grain density as a function of the specific energy loss. Table III shows the observed values of the specific energy loss  $K = -dE/dR$  in Mev/(g/cm<sup>2</sup>) and of the  $\delta$ -ray density per 100 $\mu$  track length  $n_\delta$ . It also shows the calculated values of  $K$  and  $n_\delta$  for three different assumed values of the charge  $Z$ .

Comparing the observed and calculated values we conclude that the particle was a nucleus of carbon rather than nitrogen or oxygen and that it entered the stack with an energy of 2.7 Bev ( $v/c = 0.59$ ).

### B. Particles of charge $3 \leq Z \leq 5$

These nuclei present a special problem. The  $\delta$ -ray density is too low to permit accurate charge determination unless the track is exceptionally long. The grain density of relativistic particles of charges  $Z = 3, 4$  and  $5$  is equal to that of protons of residual range 4000 $\mu$ , 1600 $\mu$  and 400 $\mu$  respectively and to that of  $\alpha$ -particles of ranges 100,000 $\mu$ , 28,000 $\mu$  and 9000 $\mu$  respectively. Thus tracks of nuclei of charge  $3 \leq Z \leq 5$  have to be sorted out from a large background of tracks of slower secondary particles, which have similar appearance. Some tracks of relativistic Li, Be and B nuclei have

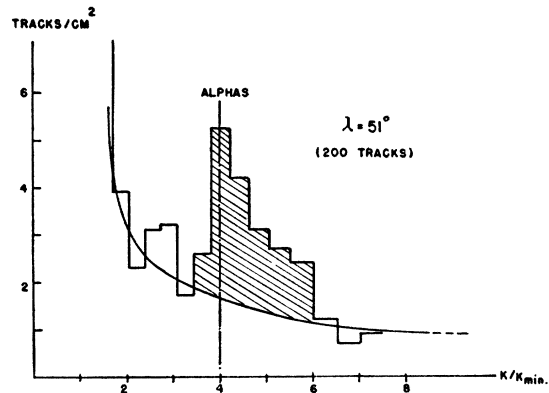


FIG. 4. Frequency distribution of 200 tracks of length  $L \geq 750\mu$  in an area  $A = 5.1$  cm<sup>2</sup> of emulsions exposed at latitude  $\lambda = 51^\circ$ , plotted against  $K/K_{min}$ . The  $\alpha$ -particle peak is broader than the corresponding peak observed at  $\lambda = 30^\circ$  (Fig. 3) extending up to about  $K/K_{min} = 6$ . Indeed, since the geomagnetic cut-off energy at  $\lambda = 51^\circ$  is only 0.5 Bev per nucleon primary  $\alpha$ -particles with a specific ionization in the interval  $K/K_{min} = 4$  to 5.5 can penetrate the earth's magnetic field.

been identified, but a systematic investigation of such tracks has not yet been carried through.

### C. The primary helium component

The difficulty connected with establishing the flux of particles of charge  $3 \leq Z \leq 5$  does not exist for particles of charge  $Z = 2$  because their number is not small compared to the number of slow secondary particle tracks with which they may be confused. The procedure used to identify the primary helium component was as follows:

(1) In an emulsion of a plate flown in Flight No. 2 for a time  $t = 22,000$  sec. at  $\lambda = 30^\circ$ , thickness  $a = 100\mu$ , sensitive to singly charged particles of all energies, all tracks which had more than 200 developed silver grains were recorded and their grain density was determined. 80 percent of all tracks so selected showed grain densities between 9 and 11 grains/75 microns, the remaining 20 percent were distributed between 11 and 80 grains/75 microns. No tracks showed a density of less than 9/75 microns. Thus minimum ionization for singly charged particles corresponds to a grain density of 10 grains/75 $\mu$  in these plates. This conclusion was verified by grain counting several pairs of thin tracks emerging from a common origin with very small angles between them (which were interpreted as due to electron-positron pairs) and also by counting the tracks in a  $\mu$ - $\beta$ -decay.

TABLE IV. Mean free path for nuclear collisions of heavy primaries in glass.

Group	Z	Number of collisions N	L cm	$\Delta L$ cm	Path length $L + \Delta L$ cm	Mean free path (gr/cm <sup>2</sup> )	
						observed	calculated
I	6-8	40	520	20	540	33 $\pm$ 5	20
II	10-18	26	255	13	269	25 $\pm$ 5	16
III	26 $\pm$ 2	8	59	3	62	19 $\pm$ 6	12

(2) An area of 5.8 cm<sup>2</sup> was surveyed for all tracks longer than 750 microns provided their grain density was larger than 18 grains/75 microns. When the number of tracks so selected is plotted *versus* their grain density, one obtains a distinct maximum at a grain density between 36 and 40/75 microns which corresponds to the minimum ionization of a particle of charge  $Z=2(K/K_{\min}=4)$ . The width of the peak is consistent with a unique value of grain density, corresponding to a specific energy loss  $K=4K_{\min}$  (Fig. 3).

The strong peak at  $K/K_{\min}=4$  could, of course, also be due to an abnormal abundance of secondary singly charged particles in the velocity range  $0.38 < \beta < 0.42$ . Such an interpretation would require an exceedingly large production in stars of particles of a particular energy (i.e., protons of 80 Mev). Not only is there no such anomaly but it can easily be shown that the peak of the distribution curve of Fig. 3 cannot be due to particles which are locally produced. We conclude that it is due to primary  $\alpha$ -particles. Its structure is consistent with a minimum  $\alpha$ -particle energy in excess of 3.5 Bev per nucleon, the minimum energy required for

the arrival of doubly charged He ions at geomagnetic latitude  $\lambda=30^\circ$ . The peak accounts for about one-fourth of all the particles of track length  $\geq L=750\mu$ , equivalent to a particle density of  $n=4.5$  alpha-particles/cm<sup>2</sup>.

The flux of alpha-particles is then equal to

$$I_0 = \frac{n}{4t\rho_L}$$

$$\text{with } \rho_L = \int_0^{\pi/2} \exp\left(\frac{-h}{\lambda \cos\vartheta}\right) \sin^2\vartheta d\vartheta$$

$$- \int_\alpha^{\pi/2} \exp\left(\frac{-h}{\lambda \cos\vartheta}\right) \sin\vartheta (\cos^2\alpha - \cos^2\vartheta)^{1/2} d\vartheta$$

and  $\sin\alpha = a/L$

$h = 16 \text{ g/cm}^2 = \text{amount of material above the plates.}$

Assuming a mean free path of  $\lambda_{\text{air}} \sim 40 \text{ g/cm}^2$  we ob-

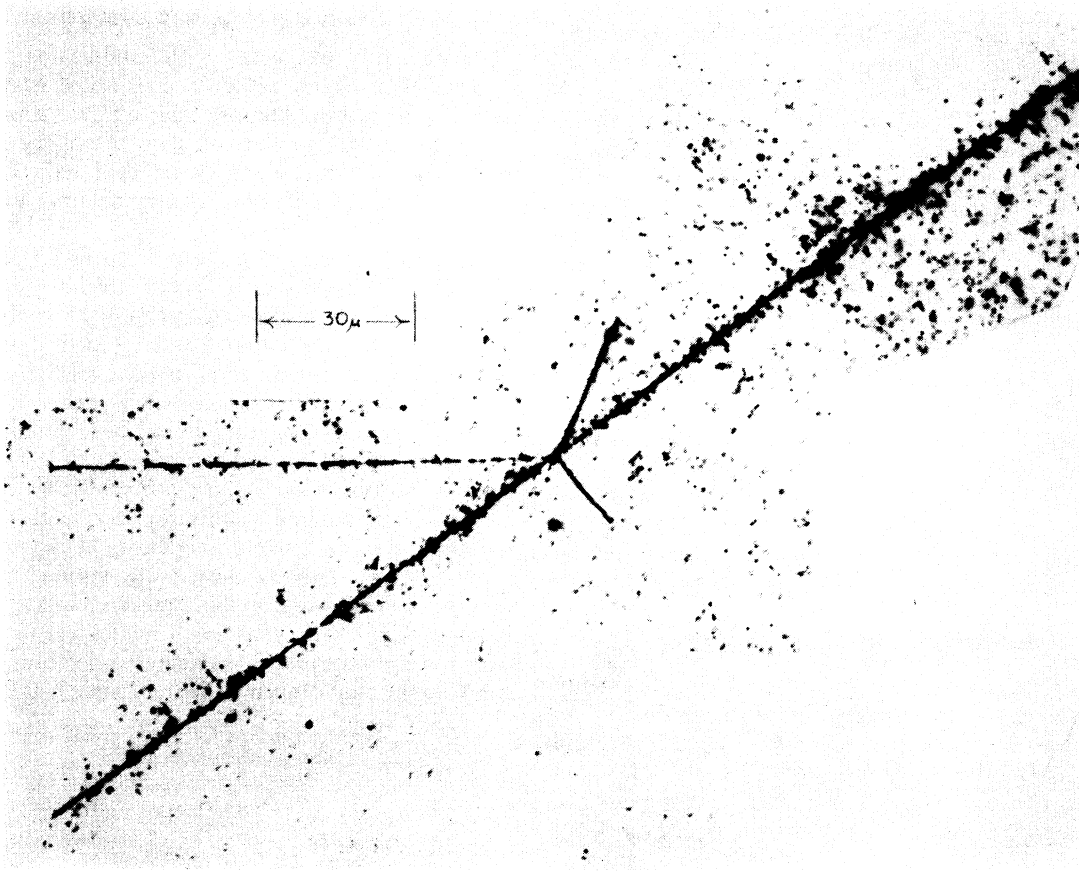


FIG. 5. A nucleus with charge  $Z \sim 20$  causes ejection of three charged particles from a target nucleus without suffering any noticeable deflection or loss of charge. This event, which was observed by Dr. E. O. Salant and Dr. J. Hornbostel, may be the result of a rather distant collision. (Courtesy of Dr. E. O. Salant and Dr. J. Hornbostel, Brookhaven National Laboratory.)

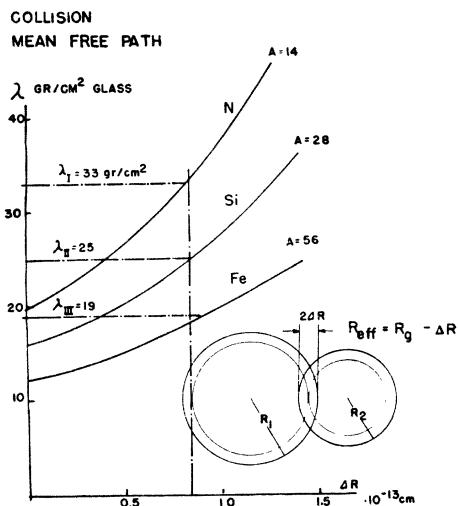


FIG. 6. Mean free path for collisions in  $\text{g/cm}^2$  glass plotted against the decrement of nuclear radius  $\Delta R = R_{\text{geom}} - R_{\text{eff}}$ . The curves are calculated for nitrogen, silicon and iron nuclei, respectively, assuming  $\lambda = 1/(\sum_i N_i \sigma_{i,\text{eff}})$  and  $R_{\text{geom}} = 1.45 \cdot 10^{-13} A^{1/2}$  cm for all nuclei involved. The observed values of the collision mean free path:  $\lambda_{\text{C,N,0}} = 33 \text{ g/cm}^2$ ,  $\lambda_{(10 \leq Z \leq 18)} = 25 \text{ g/cm}^2$ ,  $\lambda_{\text{Fe}} = 19 \text{ g/cm}^2$ , correspond to a unique value of  $\Delta R \sim 0.85 \cdot 10^{-13}$  cm.

tain for the flux at the top of the atmosphere:\*

$$I_0^{(\text{He})}(30^\circ) = (9 \pm 3) \cdot 10^{-3} \frac{\text{He nuclei}}{\text{cm}^2 \text{ sec. steradian}}$$

A similar investigation at geomagnetic latitude  $\lambda = 51^\circ$  (Flight No. 3) showed also a very distinct  $\alpha$ -particle peak of the grain density distribution curve (Fig. 4); at this latitude the peak is broadened toward higher grain densities, as one might expect at a latitude where the magnetic field permits the entrance of primary  $\alpha$ -particles with energies of only 0.5 Bev per nucleon.

For the flux of alpha-particles at the top of the atmosphere at geomagnetic latitude  $\lambda = 51^\circ$  the value

$$I_0^{\text{He}}(51^\circ) = (38 \pm 13) \cdot 10^{-3} \frac{\text{He nuclei}}{\text{cm}^2 \text{ sec. steradian}}$$

is obtained.

(3) As a further check on the interpretation of the peak given above, some individual tracks whose grain density corresponds to four times minimum ionization have been directly identified as tracks of relativistic helium nuclei. One such track, for instance, penetrated  $56 \text{ g/cm}^2$  of glass without showing any change in grain density. A proton producing a track of equal grain density would have an energy of 80 Mev and a range of only  $6.5 \text{ g/cm}^2$ . Even if the track is ascribed to a triton nucleus, the heaviest singly charged particle, the

\* This calculation is based on the assumption that the flux of particles at the top of the atmosphere is isotropic for which evidence will be presented in Section IV.

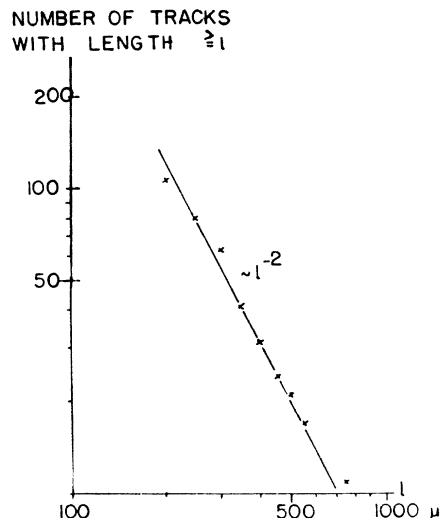


FIG. 7. Integral length distribution of 106 tracks of length  $\geq 200 \mu$  in a  $93 \mu$  thick emulsion flown at  $\lambda = 30^\circ$ . The number of tracks  $N(l)$  with length  $\geq l$  follows the expected  $1/l^2$  distribution.

range would be only  $19.5 \text{ g/cm}^2$ . On the other hand, the grain density of a track produced by a lithium nucleus would have been at least twice the observed grain density. Hence the track must have been produced by a helium nucleus of energy larger than 3 Bev.

Combined with the absolute flux values for all primary cosmic rays as obtained by J. R. Winckler *et al.* (private communication) and by M. A. Pomerantz<sup>7</sup> the  $\alpha$ -particle flux values given above indicate, that at both latitudes about 20 percent of the primaries are  $\alpha$ -particles. Pomerantz and Hereford<sup>8</sup> have concluded from their observations with low sensitivity coincidence counters that at  $\lambda = 50^\circ$  thirty percent of the primaries are  $\alpha$ -particles.

(4) Evidence for high energy  $\gamma$ -rays. In the course of this analysis of grain densities we have observed a number of tracks with a grain density corresponding to exactly twice minimum ionization. Some of them, on close inspection, proved to consist of two minimum ionization tracks originating at a point in the emulsion and diverging very slightly. Those tracks can be considered as tracks of an electron-positron pair created by an energetic  $\gamma$ -ray. Long tracks of constant grain density corresponding to twice minimum ionization are most likely unresolved tracks of electron-positron pairs whose angular divergence is smaller than our resolution ( $\vartheta \lesssim 5 \cdot 10^{-4}$  radians) produced by  $\gamma$ -rays of energy  $h\nu \gtrsim 10 \text{ Bev}$ .

One might have expected that electrons of such high energies should show a substantial relativistic increase of grain density due to the relativistic increase of specific energy loss in solids as calculated by Fermi<sup>9</sup>

<sup>7</sup> M. A. Pomerantz, Phys. Rev. **76**, 165 (1949).

<sup>8</sup> M. A. Pomerantz and F. L. Hereford, Phys. Rev. **76**, 997 (1949).

<sup>9</sup> E. Fermi, Phys. Rev. **56**, 1242 (1939); **57**, 485 (1940).



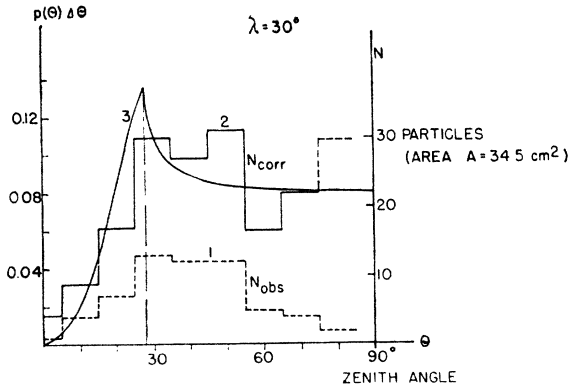


FIG. 8. Angular distribution of 60 tracks of C,N,O nuclei at  $\lambda=30^\circ$ . Histogram 1 gives the actual number of tracks with length  $\geq l=200\mu$  obtained in a systematic survey of an area  $A=34.5\text{ cm}^2$  of an emulsion of thickness  $a=93\mu$ , vertically oriented, flown for  $t=6$  hours at  $\lambda=30^\circ\text{N}$  (right scale). Histogram 2 gives the number of tracks, corrected as outlined in the text for absorption in the glass of the plates and the air overhead. Curve (3) is the geometrical factor

$$P_l(\vartheta)\Delta\vartheta = [N_{\text{corr}}(\vartheta)]/[A \cdot t \cdot I(\vartheta)].$$

It is seen that, whereas  $N_{\text{obs}}(\vartheta)$  decreases with  $\vartheta$  for large zenith angles because of the increasing absorption of the air overhead, the variation of  $N_{\text{corr}}(\vartheta)$  is within the statistical accuracy given by  $P_l(\vartheta)$ . This indicates isotropy of the radiation at the top of the atmosphere.

and Halpern and Hall.<sup>10</sup> However the sharpness of the peak for tracks with grain density corresponding to minimum grain density observed by us but also by Powell *et al.*<sup>11</sup> seems to indicate that the relativistic increase of grain density in the emulsions used is small.

In addition to what appear to be tracks of very high energy electron positron pairs we have observed the development of a larger mixed shower and cases of direct pair production by electrons (which were themselves members of a pair produced by a  $\gamma$ -ray in the emulsion).<sup>12</sup> While no quantitative work has as yet been done with nuclear emulsions on the soft component of cosmic radiation, it is evident that emulsions will prove to be useful tools for such investigations.

### III. MEAN FREE PATH FOR NUCLEAR COLLISIONS OF HEAVY COSMIC-RAY PRIMARIES

Various types of collisions of heavy primaries have been described previously (reference 5). Examples of collisions occurring in the emulsion are shown in Figs. 1,

TABLE V. Flux of heavy primaries at geomagnetic latitudes  $55^\circ$ ,  $51^\circ$  and  $30^\circ\text{N}$ .

Geom. latitude	Flight No.	$10^3 \cdot I_0 (10^3 \text{ nuclei/cm}^2 \text{ sec. steradian})$		
		$Z=2$	$6 \leq Z \leq 10$	$Z > 10$
$55^\circ$	4	—	$1.1 \pm 0.2$	$0.30 \pm 0.1$
$51^\circ$	3	$38 \pm 13$	$1.2 \pm 0.3$	$0.35 \pm 0.07$
$30^\circ$	2	$9 \pm 3$	$0.35 \pm 0.06$	$0.10 \pm 0.03$

<sup>10</sup> O. Halpern and H. Hall, Phys. Rev. 73, 477 (1948).

<sup>11</sup> Brown, Camerini, Fowler, Muirhead, Powell, and Ritson, Nature 163, 47, 82 (1949).

<sup>12</sup> H. L. Bradt, M. F. Kaplon and B. Peters, Helv. Phys. Acta (in print).

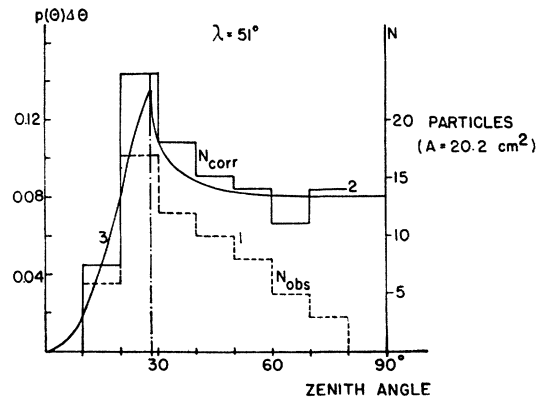


FIG. 9. Angular distribution of 61 tracks of heavy primaries at  $\lambda=51^\circ\text{N}$ .—The 61 tracks of Fig. 9 of length  $\geq l=200\mu$ , 48 of them due to C,N,O nuclei, were obtained from a complete survey of an area of  $A=20.2\text{ cm}^2$  of an emulsion of thickness  $a=90\mu$ , flown for  $t=3$  hours at geomagnetic latitude  $\lambda=51^\circ\text{N}$ . For further explanation see caption to Fig. 8.

2, 5 and 14. The mean free path in the glass of the photographic plates for collisions in which the charge of the incident primary is reduced by at least two units, has been determined separately for the nuclei of the C,N,O-group (group I), for nuclei of intermediate charge values  $10 < Z < 18$  (group II) and for nuclei of the iron group (group III).

The residual length  $l$  of all the tracks found in a systematic survey of a number of plates was measured.  $l$  is the length of track between the plate surveyed until either the point where the particle leaves the stack or the last plate where the particle is recorded before a collision occurs. Since the exact location of the collision in the glass has in general not been determined, we add in the case of a collision to the observed track length  $l$  one-half the path length in the glass before and after collision ( $\Delta l$ ). If  $L = \sum l$ ,  $\Delta L = \sum \Delta l$ , the mean free path is obtained by dividing the total track length  $L + \Delta L$  by the number of collision observed. The results are listed in Table IV.

The observed values for the mean free path, listed in column 7 of Table IV, are significantly larger than the values calculated with the assumption that the effective collision cross section  $\sigma_{\text{eff}}$  is equal to the geometrical nuclear cross section  $\sigma_{\text{geom}} (\Delta R = R_{\text{geom}} - R_{\text{eff}} = 0)$ . We estimate that with the criteria adopted for the identification of collisions (especially the systematic search for satellite tracks) only a small fraction of actual collisions in the glass would have been missed. Collisions of heavy nuclei in which neither their direction nor their charge is noticeably changed have been observed (Fig. 5),\*\* but seem to be rather infrequent.

It is conceivable that during the passage of an incident nucleus near a target nucleus some small

\*\* The event of Fig. 5 has been observed by Dr. E. O. Salant and Dr. J. Hornbostel of the Brookhaven National Laboratory. We are greatly indebted to them for pointing out to us this event and for the loan of the plate.

overlapping of the geometrical nuclear volumes may occur without causing serious damage to either projectile or target nucleus. In order to estimate whether this may possibly explain the rather large observed mean free path values, we make the crude assumption that the effective collision radius  $R_{\text{eff}}$  is equal to the geometrical radius  $R_{\text{geom}} = r_0 A^{1/3}$  ( $r_0 = 1.45 \cdot 10^{-13}$  cm) minus a certain decrement  $\Delta R$ , which may be expected to be of the order of the range of nuclear forces. If  $R$  is the geometrical radius of the incident nucleus,  $R_i$  the geometrical radius of the nucleus of kind  $i$  of the glass, we have for the collision cross section

$$\sigma_i = \pi(R + R_i - 2\Delta R)^2,$$

and for the mean free path

$$\lambda = 1/\sum n_i \sigma_i,$$

where  $n_i$  is the number of nuclei of kind  $i$  per unit volume of the glass. Figure 6 shows a plot of the values of  $\lambda$  thus calculated on the basis of the known chemical composition of the glass against the decrement of nuclear radius  $\Delta R$ . It is seen that the calculated values agree within the experimental error with the observed values  $\Delta R = 0.85 \times 10^{-13}$  cm, a decrement of nuclear radius equal to about one-half the range of nuclear forces.

#### IV. THE FLUX OF HEAVY PRIMARY COSMIC RAYS

In order to obtain the flux of particles at the top of the atmosphere, a number of plates were surveyed for tracks longer than a certain minimum length  $l$  and the zenith angle  $\vartheta$  was measured for each track. Each track within an angular interval  $\Delta\vartheta$  was given the statistical weight  $\exp[(L'/\lambda_g) + (h/\lambda_a \cos\vartheta)]$  in order to correct for the loss of particles by nuclear collisions taking place above the plate which was surveyed. Here  $L'$  is the amount of glass which the particle penetrated before it reached the plate which was surveyed,  $h$  is the amount of air above the plates,  $\lambda_g$  and  $\lambda_a \approx 0.9\lambda_g$  are the mean free paths (in g/cm<sup>2</sup>) for nuclear collisions in glass and in air, respectively, as obtained in Section III;  $\vartheta$  is the zenith angle.

After multiplying the number of tracks in a given angular interval, corrected for nuclear collisions, by the appropriate geometric factor, which depends on the orientation of the plates and the criteria used for selection, we obtain for each interval of the zenith angle the number of particles incident at the top of the atmosphere with an energy sufficient to penetrate the air above the plates. The flux at the top of the atmosphere thus calculated has been found to be within the statistical accuracy independent of the zenith angle in all cases.

As an example we shall consider the 60 tracks of length  $\geq 200\mu$  of nuclei with charge  $6 \leq Z < 10$  found in a systematic survey of  $A = 34.5$  cm<sup>2</sup> emulsion of the plates flown in Flight No. 2. The survey was made independently by two observers, which obtained essen-

tially identical results. The plane of the emulsion of thickness  $a = 93\mu$  was vertical.

Figure 7 shows the integral length distribution of 106 heavy tracks found in a systematic survey of two plates of Flight No. 2. The observed number of tracks with length  $\geq l$  follows closely the expected distribution, which is given with sufficient approximation by the relation  $N(l) \sim 1/l^2$ . This provides an additional check that indeed no appreciable number of tracks of length  $\geq 200\mu$  have been missed in the survey.

TABLE VI. Data for 30 tracks of particles stopping by ionization in the stack of 58 plates flown at Camp Ripley ( $\lambda = 55^\circ\text{N}$ ).

1	2	3	4	5	6	7	8	9
No.	Number of plates traversed by the particle	Charge $Z$	Zenith angle $\vartheta$ Degrees	Range in glass $R_g$ g/cm <sup>2</sup>	$v/c$	Total range $R$ g/cm <sup>2</sup>	Energy per nucleon $\epsilon$ Bev	Total kinetic energy $E$ Bev
1	6	6	17	13.7	0.59	33	0.39	4.7
2	5	6	34	22.7	0.66	56	0.55	6.6
3	4	6	3	41.0	0.74	60	0.57	6.9
4	2	6	49	13.6	0.59	59	0.57	6.8
5	3	6	10	14.5	0.60	30	0.37	4.5
6	6	6	32	14.1	0.60	32	0.38	4.6
7	10	6	29	17.2	0.62	34	0.39	4.7
8	6	6	18	15.8	0.61	32	0.38	4.6
9	8	6	16	24.4	0.66	40	0.44	5.3
10	9	6	26	26.2	0.67	43	0.47	5.7
11	1	6	50	9.6	0.55	32	0.38	4.6
12	6	7	30	26.0	0.71	43	0.52	7.3
13	5	8	39	11.2	0.60	30	0.45	7.2
14	3	8	31	7.8	0.56	25	0.40	6.4
15	7	8	14	24.0	0.70	40	0.53	8.5
16	4	8	12	19.0	0.67	34	0.48	7.7
17	4	10	54	7.4	0.58	33	0.54	11
18	8	11	35	11.8	0.65	26	0.50	11
19	25	12	16	69.0	0.87	85	1.20	29
20	9	12	25	16.4	0.70	35	0.63	15
21	4	12	33	12.0	0.66	30	0.57	14
22	12	12	43	26.6	0.77	42	0.71	17
23	11	14	34	18.0	0.74	36	0.71	20
24	4	14	29	29.4	0.80	89	1.40	39
25	2	14	34	13.0	0.70	31	0.65	18
26	4	20	10	5.6	0.63	21	0.62	25
27	8	22	37	5.9	0.65	25	0.76	34
28	24	26	40	35.0	0.88	55	1.45	81
29	20	26	46	24.6	0.84	48	1.30	73
30	4	26	14	22.8	0.84	38	1.10	62

The number  $\Delta N$  of tracks of length  $L \geq l$  in the interval of zenith angle between  $\vartheta$  and  $\vartheta + \Delta\vartheta$ , corrected for the loss of particles by collisions, is related to the true flux  $I(\vartheta)$ , (the number of particles per cm<sup>2</sup>, per sec. and per unit solid angle) by the relation

$$\Delta N = A \cdot t \cdot I(\vartheta) \cdot P_l(\vartheta) \cdot \Delta\vartheta,$$

where  $A$  is the area surveyed and  $t$  the time of exposure. The geometrical factor  $P_l(\vartheta)$  for vertical plate orientation and selection of tracks of length  $\geq l$  in the unprocessed emulsion is given by

$$P_l(\vartheta) = \begin{cases} 4 \sin^2\vartheta & (\vartheta \leq \alpha) \\ 4 \sin^2\vartheta \left[ 1 - \left\{ 1 - \left( \frac{a}{l \sin\vartheta} \right)^2 \right\}^{\frac{1}{2}} \right] & (\vartheta \geq \alpha), \end{cases}$$

where  $\alpha$  is given by  $\sin\alpha = a/l$ , or  $\alpha = 28^\circ$ .

TABLE VII. Breakdown of flux data for  $\lambda=30^\circ$ .

	Particles/ m <sup>2</sup> sec. steradian	%	Nucleons m <sup>2</sup> sec. steradian	%
Protons	356	79.0	356	45.0
Helium	90	20.0	360	45.3
C, N, O	3.5	.78	49	6.2
Z>10	1	.22	28	3.5
Total	450	100%	793	100%

In Fig. 8, histogram 1 represents the observed number of tracks (out of a total of 60 tracks) per  $10^\circ$  interval, plotted against the zenith angle  $\vartheta$ . Histogram 2 gives the number of tracks, as corrected for absorption in the material overhead. Curve 3 (left scale) gives the function  $P_i(\vartheta)\Delta\vartheta$ . It is seen that the variation of  $N_{\text{corr}}(\vartheta)$  with zenith angle  $\vartheta$  follows within the statistical accuracy the function  $P_i(\vartheta)$ , as would follow from an isotropic flux distribution  $I(\vartheta)=I_0$ . The falling off of the observed number of tracks with zenith angle shows the influence of the absorption of the air overhead. The absolute value of  $I_0$  is deduced from Fig. 8 to be

$$I_0 = \frac{1}{A \cdot t} \frac{N_{\text{corr}}}{P_i(\vartheta)\Delta\vartheta}$$

$$= \frac{1}{34.5 \times 2.2 \times 10^4} (275 \pm 35),$$

$$I_0(\lambda=30^\circ) = (3.5 \pm 0.6) 10^{-4} \frac{\text{C,N,O-nuclei}}{\text{cm}^2 \text{ sec. steradian}}$$

For the particles with  $Z>10$  a value for the flux at the top of the atmosphere of

$$I_0(30^\circ) = (1.0 \pm 0.3) 10^{-4} \frac{\text{nuclei with } Z>10}{\text{cm}^2 \text{ sec. steradian}}$$

is obtained.

Figure 9 shows the angular distribution of 61 tracks recorded and followed through the stack in a systematic survey of  $A=20.2$  cm<sup>2</sup> of emulsion of thickness  $a=90\mu$ , flown for  $t=3$  hours at  $\lambda=51^\circ$  (Flight No. 3). 47 tracks (77 percent) were tracks of nuclei of the C,N,O group. The criterion used for selection, hence the function  $P_i(\vartheta)$  is the same as for Fig. 8, the only difference being that for this survey the particles were required to enter the plate from the side turned away from the stack of plates. Since the same number passed the plate from the other side, the numbers of Fig. 9 have to be multiplied with a factor 2 in order to obtain the flux at the top of the atmosphere. For C,N,O nuclei we obtain

$$I_0 = 2 \cdot 0.77 \cdot \frac{(167 \pm 30)}{20.2 \cdot 1.1 \cdot 10^4}$$

$$= (1.2 \pm .3) \cdot 10^{-3} \frac{\text{C,N,O nuclei}}{\text{cm}^2 \text{ sec. steradian}}$$

The flux at the top of the atmosphere of nuclei with  $Z>10$  is about  $\frac{1}{3}$  of this value.

The flux values of heavy primary ions at the top of atmosphere are summarized in Table V.

The fact that the observed flux is within the statistical error uniform from  $\vartheta=0$  to  $\vartheta=65^\circ$  indicates that the fraction of particles with ranges between 16 g/cm<sup>2</sup> and 40 g/cm<sup>2</sup> of air is a small fraction of the total flux. This conclusion is corroborated by the observation that at  $\lambda=55^\circ$  and at  $\lambda=51^\circ$  only 10 percent of all particles stop in the stack of plates, while at  $\lambda=30^\circ$  none of the 100 particles observed stop in the stack. From this we conclude that at  $\lambda=30^\circ$  no particles enter with energies below those observable in this experiment and that the figures quoted therefore represent the true flux values at this latitude.

At  $\lambda=55^\circ$ , however, a closer analysis of the low energy part of the radiation is required.

#### V. THE LOW ENERGY PART OF THE SPECTRUM OF HEAVY PRIMARY NUCLEI AT $\lambda=55^\circ\text{N}$

At geomagnetic latitude  $\lambda=55^\circ\text{N}$  the magnetic field of the earth will not permit protons of less than  $E_0'=1.0$  Bev and completely stripped heavier nuclei ( $A=2Z$ ) of less than  $E_0^Z=0.35 \times A$  Bev to reach the atmosphere from the zenith direction.<sup>13</sup> The knee of the latitude curve observed at lower altitudes, occurring at  $\lambda=40^\circ$  for sea level observation and at  $\lambda=48^\circ\text{N}$  for observation at 25-30,000 feet altitude has in the past fre-

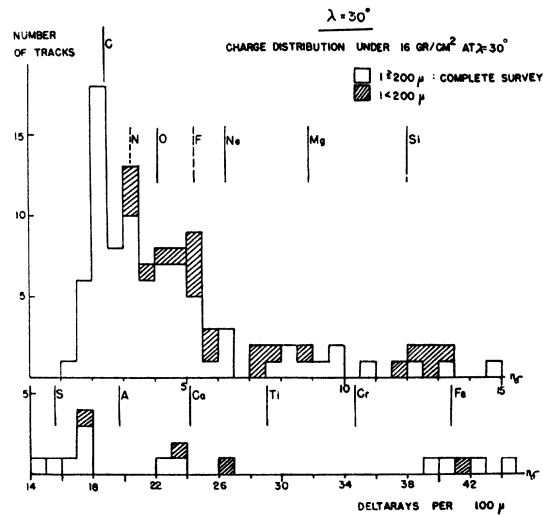


FIG. 10. Charge spectrum under 16 g/cm<sup>2</sup> air at  $\lambda=30^\circ$  (Flight No. 2).—The observed frequency of tracks with length  $l \geq 200\mu$  is plotted against their  $\delta$ -ray density (blank squares). Out of a total of 119 tracks of length  $\geq 200\mu$  found in a systematic survey, 22 are tracks of nuclei with  $Z>10$ , four of them tracks of iron nuclei.

The shaded squares represent additional tracks of length  $< 200\mu$ , found in a survey which is only representative for the higher charge values. Since the heavier nuclei are more rapidly destroyed by collisions in the material above the plates than the lighter nuclei, the charge distribution at the top of the atmosphere will show a somewhat greater proportion of the heavier nuclei than the distribution shown in Fig. 10.

<sup>13</sup> M. S. Vallarta, Phys. Rev. 74, 1837 (1948).

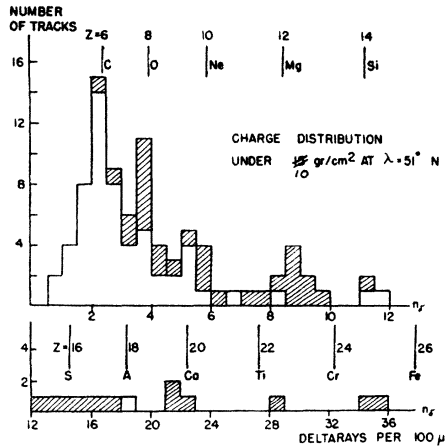


FIG. 11. Charge spectrum under 10 g/cm<sup>2</sup> of air at  $\lambda=51^\circ$  (Flight No. 3).—Of the total of 100 tracks of length  $l \geq 200\mu$ , 60 tracks result from a systematic survey of an area of 20.2 cm<sup>2</sup> of emulsion (blank squares), while the remaining 40 tracks (shaded squares) were found in a survey of 26.3 cm<sup>2</sup> which was complete only for tracks of particles with charge  $Z \geq 10$ .

quently been interpreted as an indication that the actual minimum energy of nuclei at  $\lambda=55^\circ$  N may be considerably higher than the geomagnetic cut-off for this latitude. On the other hand, if the heavy primary ions do not arrive as completely stripped ions, their geomagnetic cut-off energy would be considerably lower than the above value. For instance, the minimum energy per nucleon for penetration of the earth magnetic field at  $\lambda=55^\circ$  is  $\epsilon_0=0.35$  Bev for completely stripped carbon nuclei,  $\epsilon_1=0.15$  Bev for four times ionized carbon, and only  $\epsilon_2=0.04$  Bev for doubly ionized carbon.

In order to determine the minimum energy of heavy primaries at  $\lambda=55^\circ$  N we have selected from some 200 tracks traced through the stack flown at Camp Ripley at 97,000 ft. in Flight No. 1 a total of 30 tracks of particles which were stopped by ionization energy loss in the stack and for which the range thus could be determined. Only two of them stopped in one of the emulsions. In these cases the range can of course be very accurately measured. In general the particles stop between two adjacent glass plates. In these cases the tracks, if followed through successive plates, show increasing  $\delta$ -ray density in the last few plates before they disappear. (Disappearance of the track without any previous increase in  $\delta$ -ray density is considered to be due to a nuclear collision in the glass.) If the particle is assumed to stop in the middle between the last emulsion where the track is still seen and the following one, where the track no longer appears, the uncertainty in range  $\Delta R$  is equal to one-half the path length in one glass plate. Since most of the tracks have been followed through a great number of plates, this uncertainty is relatively small.

Table VI shows the data pertaining to these 30 tracks ending in the stack. Column 1 gives the track number, column 2 the number of plates through which

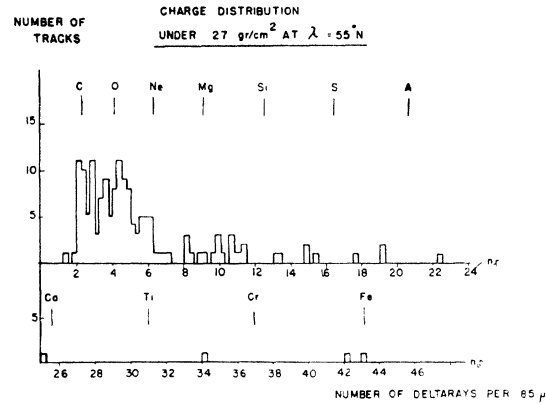


FIG. 12. Charge spectrum under 27 g/cm<sup>2</sup> of air and glass at  $\lambda=55^\circ$  (Flight No. 1).—This histogram is based on 165 tracks found in a complete survey of a given horizontal area for tracks with a projection on the vertical axis  $lz \geq 145\mu$  in 24 vertically stacked plates.

the track has been traced, column 3 the charge  $Z$  (determined by  $\delta$ -ray counting in all the plates penetrated by the particle), column 4 gives the zenith angle, column 5 the range in g/cm<sup>2</sup> glass, column 6 the velocity  $\beta=v/c$  of the particle when entering the stack of plates, column 7 the total range from the top of the atmosphere (air and glass combined), column 8 the energy per nucleon  $\epsilon$ , and column 9 the total energy at the top of the atmosphere.

The energy per nucleon  $\epsilon$  can be determined with an accuracy given by

$$\frac{\Delta\epsilon}{\epsilon} = \left[ \frac{R'}{E'} \frac{dE'}{dR'} \right] \left( \frac{\Delta Z}{Z} + \frac{\Delta R}{R} \right),$$

where  $R'$  and  $E'$  are the range and energy of a proton of equal velocity. (In the range of energies considered the quantity in the square bracket has a numerical value between 0.6 and 0.8.)  $(\Delta Z)/Z$  and  $(\Delta R)/R$  are the percentage error in the charge determination and the range determination respectively. In most cases  $\epsilon$  can be obtained with an accuracy better than 10 per cent.

In Figs. 2 and 3 of a preliminary communication<sup>14</sup> we have plotted the kinetic energies of these 30 particles stopping in the stack against their charges, and also the frequency of tracks against the energy per nucleon. As is seen also from Table VI energies per nucleon as low as  $\epsilon=0.37$  Bev occur for the lighter ions, for which the energy necessary for penetrating the material above the plates is smaller than the geomagnetic cut-off energy for stripped nuclei  $\epsilon_0=0.35$  Bev. This minimum energy amounts to 0.25 Bev per nucleon for carbon nuclei incident from the zenith. Actually, about one-half of the 16 nuclei of the C,N,O group stopping in the stack have energies per nucleon

<sup>14</sup> H. L. Bradt and B. Peters, Phys. Rev. **76**, 156 (1949).

in the interval 0.37–0.45 Bev, while none has been observed with energy below 0.35 Bev per nucleon.

If this apparent energy cut-off at  $\epsilon=0.37$  Bev is real, it would indeed strongly indicate that the C,N,O nuclei are completely stripped of electrons before they enter the earth's magnetic field (and are therefore subject to the full influence of this field). The fact that energies down to the geomagnetic cut-off actually occur would then indicate that up to latitudes as high as  $\lambda=55^\circ$  the lower energy limit is actually determined by the earth's field (see also Freier, Ney, and Oppenheimer<sup>15</sup>). An upper limit for the sun's magnetic field could thus be deduced.

However, the number of low energy C,N,O nuclei recorded at  $\lambda=55^\circ$  is still small and furthermore the upper few centimeters of the stack of plates of Flight 1 were of uneven sensitivity, a fact which discriminated somewhat against observing particles with energies per nucleon below 0.3 Bev. Though it therefore, may not be entirely safe to draw any definite conclusions about the solar magnetic field from the data presented in Table VI, it is clear that this type of measurement, especially when carried out at higher latitudes and greater altitudes should give useful information on the strength of the sun's magnetic field.

Additional evidence that at least the nuclei with atomic numbers  $Z < 10$  are completely stripped of elec-

trons when entering the earth's magnetic field is deduced from the fact that none of the 150 completely analyzed nuclei stop in the stack flown at  $\lambda=30^\circ$ . For, if C,N,O nuclei are not completely stripped, we must expect that the very heavy nuclei retain most of their electrons and are therefore not prevented by the earth's field to enter even at  $\lambda=30^\circ$  with energies sufficiently low to be stopped in the stack of plates flown in Flight 2. This is not the case for any of the still small number of very heavy particles observed so far in the stack of plates flown at  $\lambda=30^\circ$ .

At  $\lambda=55^\circ$ , about 8 percent of all the particles entering the stack of plates flown in Flight No. 1 were stopped by ionization energy loss in the stack. At  $\lambda=51^\circ$  about 7 percent of the particles entering the smaller stack flown in Flight No. 3 were stopped in it by ionization energy loss (17 tracks of particles stopped in the stack in a surveyed area of 80 cm<sup>2</sup> (0.21 tracks/cm<sup>2</sup>) as compared to a total of 60 heavy tracks in a surveyed area of 20.2 cm<sup>2</sup> (3 tracks/cm<sup>2</sup>)). The energies of most of the stopped particles lie in the interval between  $E_c$  and  $2E_c$  ( $E_c$ =geomagnetic cut-off energy).

#### VI. THE CONTRIBUTION OF HEAVY PRIMARY NUCLEI TO THE TOTAL PRIMARY AND SECONDARY RADIATION

A discussion of the contribution of heavy primary nuclei to the total primary and secondary radiation

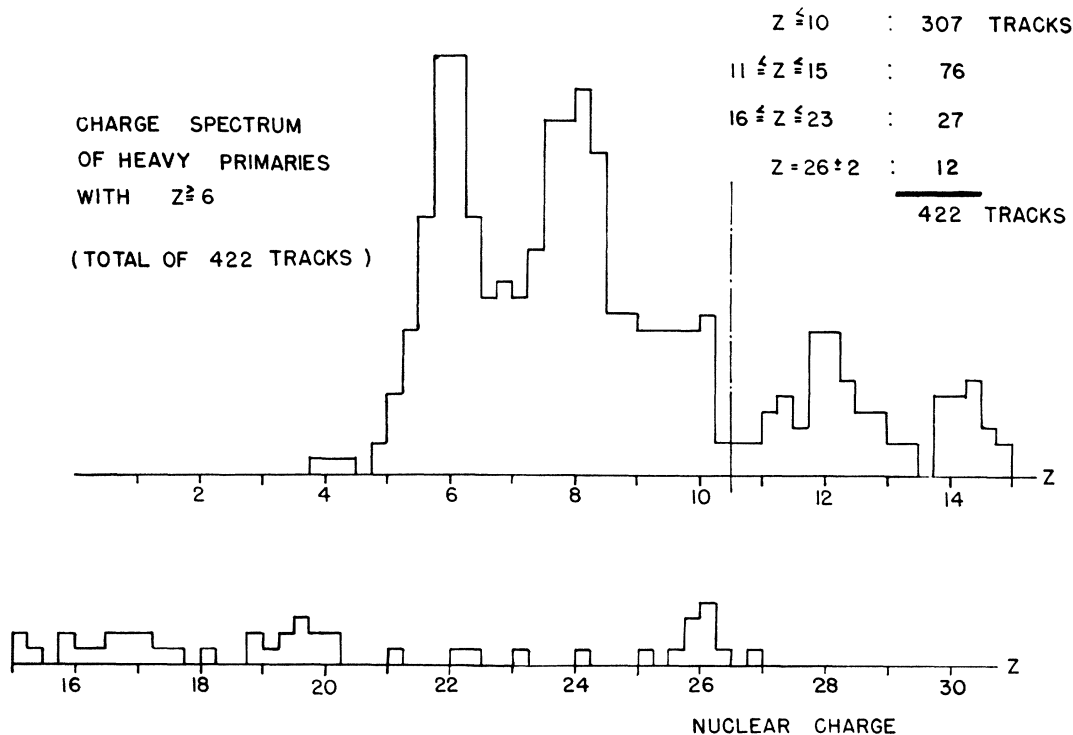


FIG. 13. Charge spectrum of heavy primaries with charge  $Z \geq 6$ .—The 422 tracks on which this graph is based are the total of all tracks which have been followed through the stacks of Flights 1, 2 and 3 for which a reasonably accurate charge determination could be made. No nuclei with charge  $Z > 26$  were found. The graph is representative only for  $Z \geq 6$  since the surveys excluded tracks which appeared significantly lighter than tracks of carbon nuclei.

<sup>15</sup> Freier, Ney, and Oppenheimer, Phys. Rev. 75, 991 (1949).

should be based on the data obtained at  $\lambda=30^\circ$  for the following reasons:

A. The absence of low energy particles indicates that our flux data, extrapolated to the top of the atmosphere, represent the entire heavy primary radiation.

B. The flux at this latitude has been determined for all masses from helium to iron (except for Li, Be, B).

C. A reasonably close upper limit can be given for the total primary flux using the data obtained by J. R. Winckler.

We shall use for the primary flux at  $\lambda=30^\circ$  a value of 450 particles per square meter, sec. and steradian.

Using the flux data for  $\lambda=30^\circ$  quoted above the breakdown summarized in Table VII is obtained.

Thus one-half of the incoming nucleons are contained in the incident heavy nuclei and one-quarter of the total number of incoming nucleons are neutrons.

If the nuclei are stripped of electrons, their energies must exceed the geomagnetic cut-off energy at  $\lambda=30^\circ$  of  $\epsilon_0=3.5$  Bev per nucleon. The energy lost by ionization per mean free path for collision is, on the other hand, equal to: for protons 170 Mev, for nitrogen 180 Mev/nucleon, for silicon 260 Mev/nucleon, for iron 330 Mev/nucleon, and therefore represents for all nuclei only a small fraction of their energy.

Thus most heavy primaries are destroyed in nuclear collisions long before they could be stopped by ionization and hence they ought to be responsible for about one-half of the secondary radiation observed at lower altitudes.

This leads to the conclusion that since the total cosmic-ray intensity at sea level shows only minute diurnal and seasonal variation, the same must be true for that part of the heavy component which is energetic enough to penetrate the earth field at  $\lambda=30^\circ$ .

#### VII. THE LATITUDE EFFECT OF THE HEAVY PRIMARY RADIATION AND ITS ENERGY SPECTRUM

The last conclusion makes it legitimate to compare results at different latitudes although the measurements were made at different times.

In comparing the flux data obtained at  $\lambda=55^\circ-51^\circ$  and  $\lambda=30^\circ$  we observe that the ratio of the number of nuclei of the carbon, nitrogen, oxygen group to the number of nuclei of charge  $Z>10$  is within the experimental error the same at both latitudes. Therefore the velocity spectra of these two groups are similar at least up to energies of 5-10 Bev per nucleon. Comparing the absolute numbers at the two latitudes, we find that the latitude effect between latitudes  $50^\circ$  and  $30^\circ$  amounts to about a factor 3.5.\*\*\* In addition, we

\*\*\* As a result of an oversight in the evaluation of the data, the flux value for heavy primaries at  $\lambda=55^\circ$  given in a preliminary communication (reference 14) is considerably too low. Since the value for  $\lambda=30^\circ$  is correct, the latitude effect has unfortunately been underestimated in this note. The value  $I_0(51-55^\circ):I_0(30^\circ)=3.5:1$  for the ratio of the numbers of heavy primaries at  $\lambda=51-55^\circ$  and at  $\lambda=30^\circ$  is in good agreement with the value  $(3.6\pm 0.4)$  obtained for the ratio of the numbers of big stars in photographic emulsions by E. O. Salant and J. Hornbostel (private communication).

TABLE VIII. Relative abundance of the nuclei of the light elements in stellar atmospheres (Unsold) and in the primary cosmic radiation at  $\lambda=30^\circ$ .

Z	Element	Sun	Stellar atmospheres (Unsold)*	Cosmic radiation at $\lambda=30^\circ$
1	H		$1.6 \cdot 10^6$	$1.6 \cdot 10^6$
2	He		$2.9 \cdot 10^6$	$4.0 \cdot 10^6$
6	C	550	280	
7	N	1150	620	
8	O	1500	1600	
	Total $6 \leq Z \leq 8$	3200	2500	14000
10	Ne		1800	
11	Na	5	2	} $\sim 4000$
12	Mg	81	107	
13	Al	6	6	
14	Si	55	100	
	Total $11 \leq Z \leq 14$	157	215	$\sim 2600$
16	S	23	} ?	$\sim 1000$
18	A			
20	Ca	5		
26	Fe	150		$\sim 400$

\* Abundance of Si = 100 in  $\tau$ -Scorpii. The table contains all the elements with abundance greater than 5 percent of the abundance of Si.

estimate that some 10 percent of the particles observed at  $\lambda=55^\circ$  and  $\lambda=51^\circ$  geomagnetic latitude have energies between the cut-off energy and twice the cut-off energy (0.35-0.7)(Bev/nucleon) at  $\lambda=55^\circ$  and (0.5-1.0)(Bev/nucleon) at  $\lambda=51^\circ$ .

Both these observations are consistent with an energy spectrum for the heavy primaries  $\mathcal{F}(\epsilon)$ , which for low energies increases with energy up to a maximum in the neighborhood of  $\epsilon_m=2.0$ (Bev/nucleon) (same magnetic rigidity as a 5 Bev proton) and falls off beyond this maximum as  $1/\epsilon^{2.5}$ . Whether or not a maximum actually occurs,  $\mathcal{F}(\epsilon)$  certainly cannot decrease with energy as rapidly as  $\epsilon^{-2.5}$  near the geomagnetic cut-off at  $\lambda \approx 50^\circ$ . A change in slope of the energy spectrum around 4 Bev is indicated for the total primary radiation by the observations of Millikan<sup>16</sup> and co-workers and by the change of the slope of the latitude curve of cosmic rays at 30,000 feet as geomagnetic latitude  $\lambda=48^\circ$ , observed by W. F. G. Swann and co-workers.<sup>17</sup>

Flights at different latitudes are needed in order to obtain more definite information on the shape of the energy spectrum of the heavy primaries.

A detailed comparison of the energy distribution of primary protons with that of heavy primaries may throw some light on the accelerating mechanism of cosmic rays. The low energy part of the spectrum can be investigated by measuring charge and range simultaneously as discussed in reference.<sup>2</sup> This method is not applicable for energies much higher than 1 Bev/nucleon since at these energies almost all particles will

<sup>16</sup> R. A. Millikan, Rev. Mod. Phys. 21, 1 (1949).

<sup>17</sup> W. F. G. Swann *et al.*, Fifth Semi Annual Report Bartol Research Foundation (March 1949).

undergo nuclear collisions rather than come to rest by ionization.

In the range from 1–10 Bev/nucleon an integral spectrum could be obtained from the latitude effect and the East-West asymmetry of the radiation.

The frequency of occurrence of even higher energies may be estimated from collisions of the type illustrated in reference 5.

#### VIII. THE RELATIVE ABUNDANCE OF NUCLEI OF THE DIFFERENT ELEMENTS IN THE PRIMARY RADIATION

Figures 10, 11 and 12 show histograms of the charge spectrum for charges  $Z \geq 6$  as observed in the plates flown at latitudes  $\lambda = 30^\circ$ ,  $\lambda = 51^\circ$ , and  $\lambda = 55^\circ$ , respectively, below 16, 10, and 27 g/cm<sup>2</sup> of air. Since the fraction of heavy elements destroyed in the material above the plates is larger than the corresponding fraction of light elements, the actual charge spectrum at the top of the atmosphere will show a somewhat higher percentage of the heavier elements than the histograms.

Figure 13 shows the frequency distribution of 422 tracks of nuclei with charge  $Z \geq 6$  (practically all the nuclei for which the charge has been determined with any accuracy) plotted against the nuclear charge. Although this diagram contains a number of tracks which were not found in systematic surveys (mainly tracks of nuclei with charge  $Z \geq 10$ ), it is believed to be fairly representative of the actual charge spectrum of incoming nuclei above  $Z = 6$ . The number of nuclei with  $Z > 10$  in Fig. 13 is about one-third of the C,N,O group. Hence it seems that the emphasis given to the heavier nuclei by inclusion of a number of tracks from non-systematic surveys roughly compensates the deficiency due to the stronger absorption of the very heavy nuclei in the air above the plates.

Although the charge determinations are not accurate enough to permit to distinguish one element from its immediate neighbors for  $Z \approx 10$ , we can nevertheless draw the following conclusions:

A. The similarity of the spectra obtained at the different latitudes indicates that the velocity spectra of the nuclei from helium to iron are not radically different, if they differ at all. This suggests that the accelerating mechanism does not depend critically on the mass of ions for which the ratio of charge to mass  $Z/M$  is approximately equal.

B. Particles of atomic number higher than the one corresponding to elements in the neighborhood of iron have not been observed. This fact seems to be significant in view of the astrophysical data on the relative abundance of elements in stellar atmospheres, which show that iron is the heaviest element with an abundance comparable with the abundance of the lighter elements.

C. About  $\frac{2}{3}$  of all the nuclei with charges  $\geq 6$  belong to the group  $6 \leq Z \leq 10$ , which we call the C,N,O group, since most of the nuclei of this group are certainly nuclei of carbon, nitrogen, and oxygen. The abundance of carbon and oxygen seems to be approximately equal and greater than that of nitrogen. It is difficult to estimate the actual abundance of nitrogen because the carbon and oxygen peaks overlap (Fig. 13). Though charges below 10 may be identified uniquely in favorable cases (see Table III), the resolution shown in Figs. 10–13 is poor even for this group; but the histograms indicate, nevertheless, that the number of nuclei with charges  $Z = 9$  or 10 cannot be insignificant.

A determination of the relative abundance of these nuclei would be especially important, because different assumptions on the origin of cosmic rays may give quite different abundance values for these nuclei. The cosmic abundance of fluorine seems to be very small and F nuclei might occur only as breakup products of heavier nuclei. The same would be true for neon if one assumes a specific accelerating mechanism as for instance that suggested by Spitzer.<sup>6</sup>

D. Of the nuclei with charges  $Z > 10$  about 60 percent belong to the Mg-Si group ( $11 \leq Z \leq 15$ ) and some 10 percent to the iron group ( $Z = 26 \pm 2$ ).

The following Table VIII lists the relative flux values of the cosmic-ray primaries together with the relative abundances of nuclei in the atmosphere of the sun and  $\tau$ -Scorpii according to Russell and Unsold.<sup>18</sup>

There is obviously considerable similarity between these relative abundances, though some differences appear: for instance, the abundance ratio of the metals with respect to He (same  $Z/M$ ) in the cosmic radiation is *ca.* 10 times greater than in stellar atmospheres. This difference seems to be outside the quite considerable possible error of the figures listed above. (The uncertainty of the astrophysical data is estimated by Unsold to be of the order of a factor two.)

#### IX. REMARKS ON THE ORIGIN OF COSMIC RADIATION

A. If we assume with Alfvén<sup>19</sup> and Richtmeyer and Teller<sup>20</sup> that cosmic rays are accelerated in the neighborhood of the sun and if we further assume that they hit the earth after circling the planetary system during a time short as compared to the time between collisions with interstellar hydrogen atoms, then we would expect that the relative proportion in which particles of different mass are accelerated is the same proportion in which they appear in the cosmic radiation.\*\*\*\* Because of the high ionization potential of He and H, the relative proportion of neutral and ionized helium and hydrogen atoms, which is very large at the solar surface, may possibly even be large in those regions near the sun where acceleration starts, whereas the metal atoms are strongly ionized even in the solar atmosphere. This may be the cause for an excess of heavy nuclei in the initial stages of the acceleration. On the other hand until the heavy atoms have obtained sufficient energy to lose all their orbital electrons their ratio of charge to mass is less than that for helium and it is always less than that for hydrogen. Thus, at some

<sup>18</sup> A. Unsold, *Zeits. f. Astrophys.* **21**, 1 (1944); **24**, 306 (1946).

<sup>19</sup> H. Alfvén, *Phys. Rev.* **75**, 1732 (1949).

<sup>20</sup> R. D. Richtmeyer and E. Teller, *Phys. Rev.* **75**, 1729 (1949).

\*\*\*\* Whether the break up of heavy nuclei in interstellar space is important could be tested by studying the relative abundance of the nuclei of certain elements. Nuclei of Li, Be and B, the light elements of extremely low cosmic abundance are expected to occur; if at all, only as products of the break up of heavier nuclei. If Li, Be and B nuclei are produced by the break up of heavier primaries in the earth's atmosphere only, as would be expected in the case of solar origin of cosmic rays, then the intensity *vs.* altitude curve for these nuclei should be a transition curve extrapolating to intensity zero at the top of the atmosphere. On the other hand, if break up of heavier nuclei in interstellar space is important, as it must be if cosmic rays are of galactic origin, then this curve is expected to extrapolate to a finite intensity at the top of the atmosphere.

stage of the accelerating process, hydrogen should be favored and even helium may be accelerated more efficiently than heavier ions. Hence, the observed charge distribution may well be consistent with the hypothesis that cosmic rays originate near the sun.

B. Let us assume that cosmic rays are accelerated in the galaxy and that there exists in the galaxy domains with magnetic fields of the order of  $H \sim 10^{-5}$  gauss, as postulated by Alfvén and by Fermi.<sup>21</sup> The hypothesis of the existence of such magnetic domains has recently received empirical support by the discovery of the polarization of starlight passing through interstellar clouds, observed by Hall<sup>22</sup> and Hiltner<sup>23</sup> and discussed by Spitzer and Tukey.<sup>24</sup> Thus nuclei accelerated to cosmic-ray energies would be either completely retained in the galaxy or at least execute long and tortuous paths through interstellar space. Collisions with nuclei of interstellar hydrogen will eventually destroy the cosmic-ray primaries or reduce their energy. Because of their much larger cross section, the heavy primaries will be eliminated by these collisions much faster than the protons.

Figure 14 shows an event which is very probably the break up of a heavy primary ( $Z=10 \pm 1$ ) in a collision with a hydrogen target nucleus. The collision of Fig. 14 is remarkable insofar as it is the only case observed of a collision of a heavy primary where no visible low energy particles are emitted from the target nucleus. It is therefore not improbable that this latter has been a hydrogen nucleus of the emulsion. (The projected hydrogen target nucleus may actually be the particle responsible for track 4.) If this is the case, Fig. 14 is an illustration for the break up of heavy cosmic-ray primaries in collisions with interstellar hydrogen atoms.

It is noteworthy that, even if we make the extreme assumption that originally *only* heavy nuclei such as iron, calcium, silicon, oxygen and carbon are accelerated, we can nevertheless account for the observed abundance of protons and  $\alpha$ -particles in cosmic radiation as fragments of collisions suffered by the heavy nuclei in interstellar space.

The cross section for collision between a relativistic nucleus of iron, calcium or silicon and a proton is of the order of  $\sigma_M = 0.3 \times 10^{-24}$  cm<sup>2</sup>. With a mean density of interstellar hydrogen in our galaxy of  $\rho = 10^{-24} - 10^{-25}$  g/cm<sup>3</sup> this corresponds to a mean life of these nuclei in the galaxy of  $\tau_M = 3 \times 10^6 - 3 \times 10^7$  years. Therefore the injection mechanism must be capable of reproducing the heavy nuclei in the cosmic radiation at the rate of about once every 10 million years. Heavy nuclei will finally be reduced by collisions to  $\alpha$ -particles, protons and neutrons (which in turn decay into protons). According to our observations on the collision of heavy

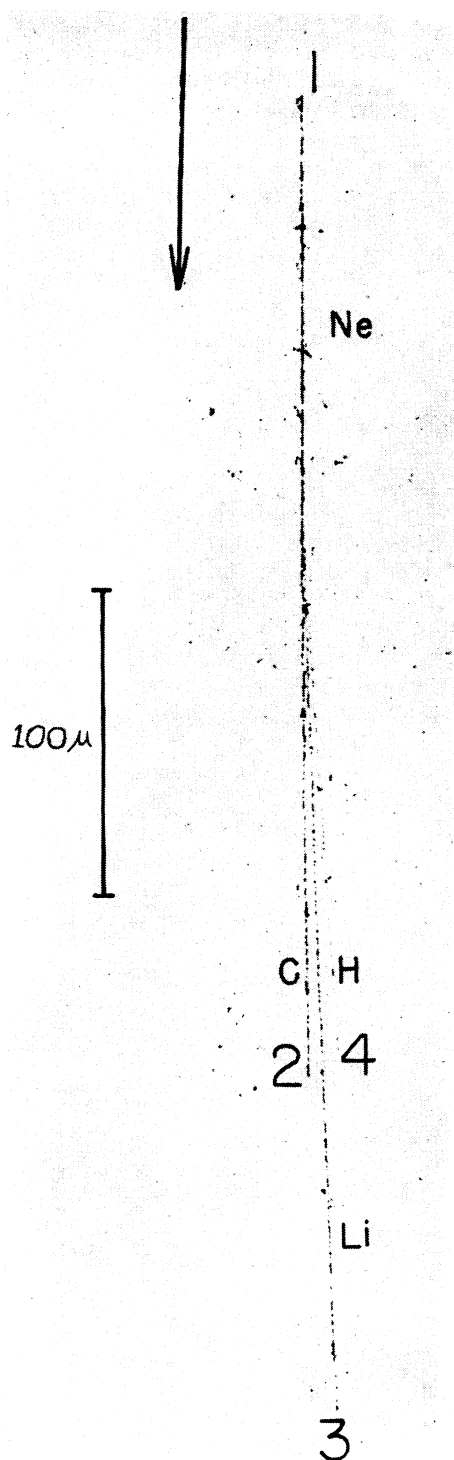


FIG. 14. A heavy primary nucleus of charge  $Z=10 \pm 1$  (track No. 1), after traversal of seven plates ( $7.5$  g/cm<sup>2</sup> of glass) is split up in the emulsion of the eighth plate into at least two fragments, one of charge  $Z=6$  or  $7$  (track No. 2) and one of charge  $Z=3$  (track No. 3) diverging with an angle of  $1.5^\circ$ . Track No. 4 is a track with grain density corresponding to a specific energy loss  $K/K_{\text{min}}=2.2$  and is probably caused by a proton of  $200$  Mev. All three tracks 2, 3, and 4 have been traced through the next plate.

<sup>21</sup> E. Fermi, Phys. Rev. **75**, 1169 (1949).

<sup>22</sup> J. S. Hall, Science **109**, 166 (1949).

<sup>23</sup> W. A. Hiltner, Science **109**, 165 (1949).

<sup>24</sup> L. Spitzer and J. W. Tukey, Science **109**, 461 (1949).



primaries in photographic emulsions even a nucleus as heavy as iron will be reduced to protons, neutrons and  $\alpha$ -particles in not more than  $\sim 3$  collisions.

We shall now discuss the extreme assumption that *only* heavy nuclei of charge  $Z \geq 6$  are originally accelerated in the galaxy and calculate the number of  $\alpha$ -particles and protons which result from the break-up of these nuclei and are expected to accompany the heavy component of cosmic radiation which will hit the earth if equilibrium is established. Let us start originally with 7 fast nuclei of carbon, nitrogen, and oxygen and 2 fast nuclei, heavier than oxygen with an average atomic weight of  $A=30$ , designated hereafter with the symbol  $M$  (metals). This represents the relative intensity of heavy nuclei with energies above 3.5 Bev/nucleon ( $\lambda=30^\circ$ ).

The break-up products of such nuclei when colliding with protons are known from the probability of occurrence of different star fragments produced by fast protons in photographic emulsions. There, about 50 percent of the slow charged fragments are  $\alpha$ -particles.<sup>25</sup> Thus  $A/6$   $\alpha$ -particles and  $A/3$  protons and neutrons result from the breaking up of a nucleus of mass number  $A$ . This will also be the ratio of fast  $\alpha$ -particles to fast protons produced in collisions of energetic heavy nuclei with hydrogen nuclei in interstellar space, since both processes are identical in the appropriate reference systems.

The life time of each nuclear component will be proportional to its cross section for collision with interstellar hydrogen nuclei.

For the inelastic collision cross section of protons with protons we take

$$\sigma_p = 0.02 \times 10^{-24} \text{ cm}^2.$$

For the cross section which leads to the break up of a helium nucleus in collision with a hydrogen nucleus we take

$$\sigma_{\text{He}} = 4\sigma_p = 0.08 \times 10^{-24} \text{ cm}^2.$$

The cross section for the destruction of a nucleus of the C,N,O-group in collision with hydrogen can be obtained from the known absorption cross section of primary cosmic rays in air. A mean free path for the absorption of primary protons in air of  $\lambda=100$  g/cm<sup>2</sup> gives the cross section

$$\sigma_{\text{C,N,O}} = 0.20 \times 10^{-24} \text{ cm}^2.$$

The collision cross section for nuclei of atomic weight  $A \sim 30$  can be estimated from the absorption of star producing radiation in aluminum<sup>26</sup> to be

$$\sigma_M = 0.3 \times 10^{-24} \text{ cm}^2.$$

We therefore obtain for the number of fast  $\alpha$ -particles ( $N_{\text{He}}$ ) in equilibrium with nuclei of charge  $Z \geq 6$

$$N_{\text{He}} = \frac{14}{6} \frac{\sigma_{\text{CNO}}}{\sigma_{\text{He}}} N_{\text{CNO}} + \frac{30}{6} \frac{\sigma_M}{\sigma_{\text{He}}} N_M \approx 80$$

<sup>25</sup> J. B. Harding, Phil. Mag. **11**, 530 (1949).

<sup>26</sup> G. Bernardini, Phys. Rev. **75**, 1328 (1949).

and for the number of fast protons ( $N_p$ )

$$N_p = \frac{14}{3} \frac{\sigma_{\text{CNO}}}{\sigma_p} N_{\text{CNO}} + \frac{30}{3} \frac{\sigma_M}{\sigma_p} N_M + 4 \frac{\sigma_{\text{He}}}{\sigma_p} N_{\text{He}} \approx 1900$$

Thus on the assumption that only nuclei of charge  $Z \geq 6$  are accelerated we predict that the ratio of elements in cosmic radiation with energies above a certain minimum energy per nucleon should be

$$\text{H:He:C,N,O:} Z \geq 10 = 1900:80:7:2.$$

Since collision products of relativistic nuclei have roughly the same velocity, hence the same energy per nucleon as the original nucleus the calculated ratios should be compared with the relative fluxes above a given energy per nucleon. Thus if we take for nuclei heavier than H the flux values at geomagnetic latitude  $\lambda=30^\circ$  (cut off energy  $\epsilon_c=3.5$  Bev per nucleon) we must compare them with the proton flux at latitude  $\lambda=42^\circ$  where the cut-off energy  $\epsilon_1$  for protons is also 3.5 Bev. Assuming a latitude effect of 1.7 for the proton component between  $\lambda=42^\circ$  and  $\lambda=30^\circ$ , the observed ratio of fluxes is

$$\text{H:He:C,N,O:} Z \geq 10 = 1200:180:7:2.$$

The comparison shows that the acceleration of heavy nuclei *only* would lead to a flux of protons and  $\alpha$ -particles in cosmic radiation which is of the correct order of magnitude.

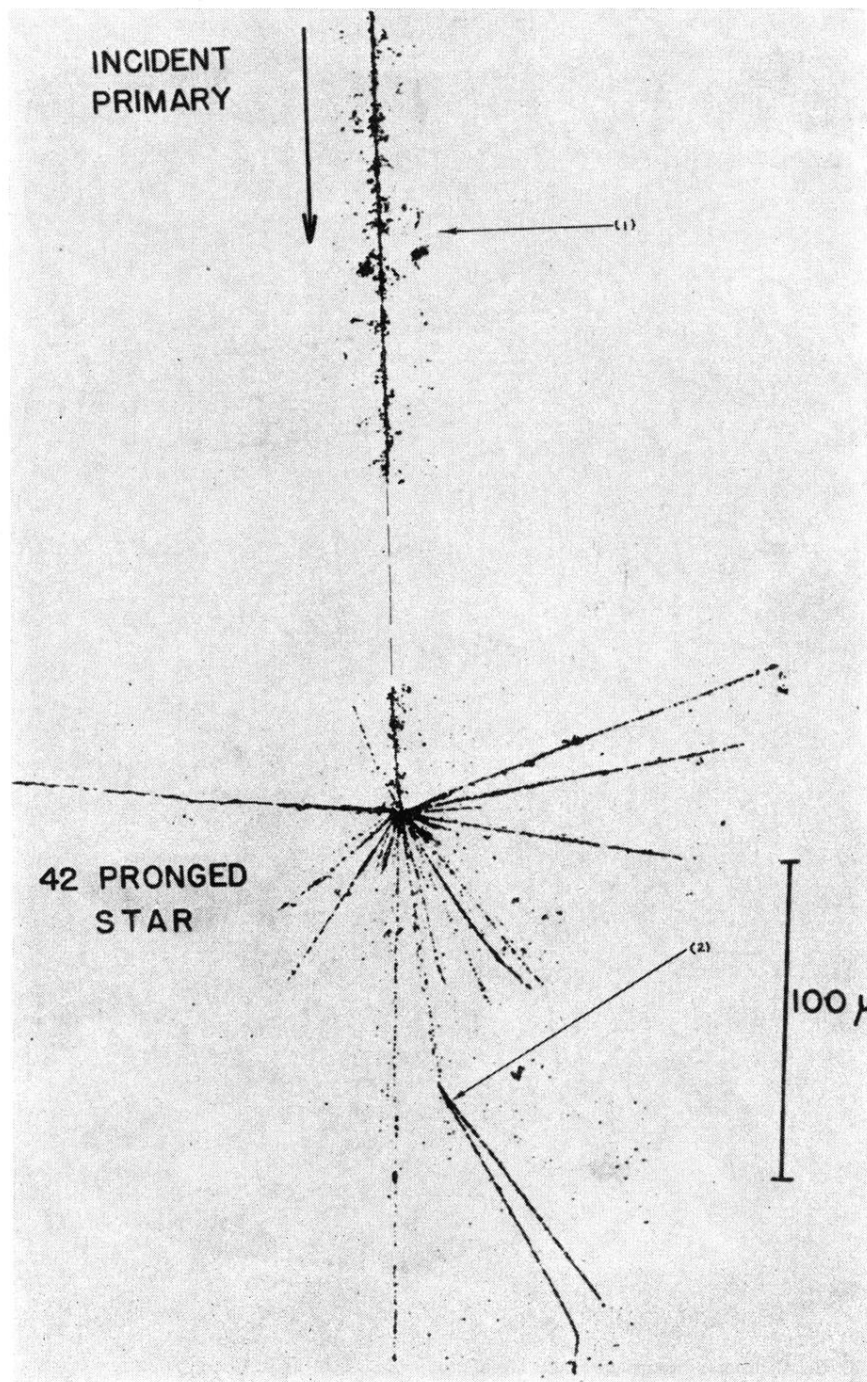
A direct acceleration of protons and helium nuclei in addition to heavy nuclei is consistent with the observations only if the number of *nucleons* accelerated as protons or  $\alpha$ -particles is at most of the same order as the number of nucleons accelerated as heavy nuclei.

The conclusion that, assuming equilibrium in the galaxy to be established, the number of hydrogen and helium nuclei cannot be significantly greater than the number of nuclei in heavier atoms injected in the accelerating process, is difficult to understand if cosmic rays originate as ions accelerated by electromagnetic fields in regions of the galaxy where hydrogen is predominantly ionized. If, on the other hand, a mechanism like that proposed by Spitzer<sup>6</sup> should be considered acceptable by means of which only heavier atoms could be accelerated to cosmic-ray energies in the galaxy, the hydrogen and helium nuclei could be accounted for as fragments from collisions with hydrogen nuclei in interstellar space.

We are greatly indebted to Mr. Robert Brent and Mr. Robert Rickard, who did most of the surveying and  $\delta$ -counting, to Mr. Lionel Goldfarb who helped carry out the  $\alpha$ -particle work and to Mr. Tom Putnam, who prepared the photographs.

We also wish to express our gratitude to Dr. John Spence of Eastman Kodak Company and Drs. E. O. Salant and J. Hornbostel of the Brookhaven National Laboratory for making available to us their facilities in many important phases of this work. This work was assisted by the Joint Program of the ONR and the AEC.

FIG. 1. Collision of a primary Ca nucleus ( $Z=20\pm 1$ ) with an energy of the order of at least 100 Bev and an Ag or Br nucleus of a Kodak NTB3 emulsion, flown in Flight No. 2 at  $\lambda=30^\circ\text{N}$ . 42 charged particles are emitted in this violent explosion. 10 prongs are minimum ionization tracks, collimated in the forward direction (they are hardly visible in Fig. 1); most of them probably are tracks of a meson shower. One fast, singly charged particle causes a second nuclear event (2).



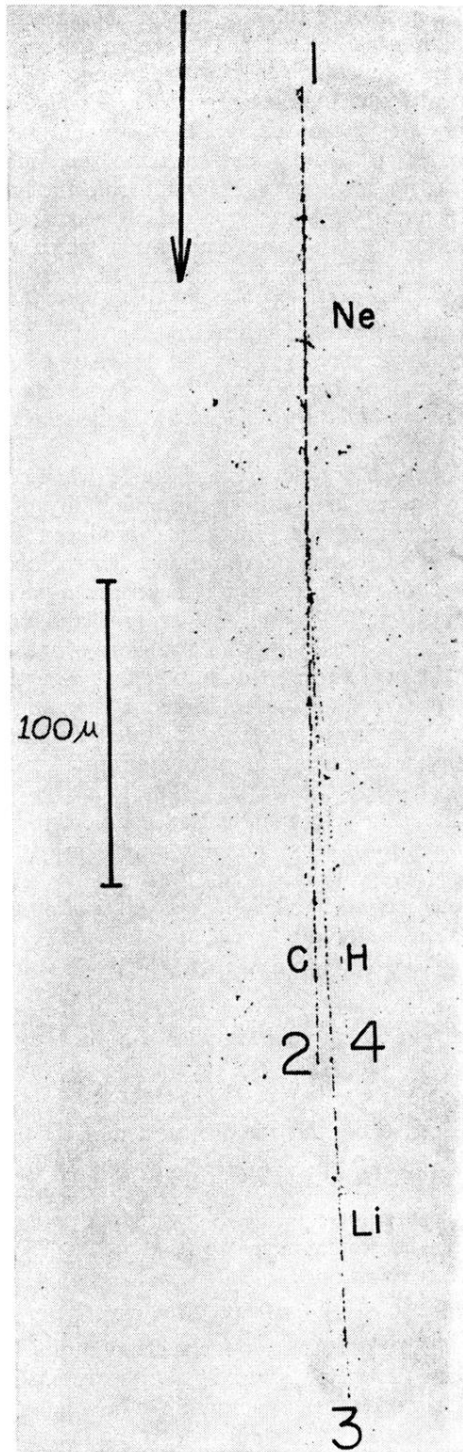


FIG. 14. A heavy primary nucleus of charge  $Z=10\pm 1$  (track No. 1), after traversal of seven plates ( $7.5 \text{ g/cm}^2$  of glass) is split up in the emulsion of the eighth plate into at least two fragments, one of charge  $Z=6$  or  $7$  (track No. 2) and one of charge  $Z=3$  (track No. 3) diverging with an angle of  $1.5^\circ$ . Track No. 4 is a track with grain density corresponding to a specific energy loss  $K/K_{\text{min}}=2.2$  and is probably caused by a proton of 200 Mev. All three tracks 2, 3, and 4 have been traced through the next plate.

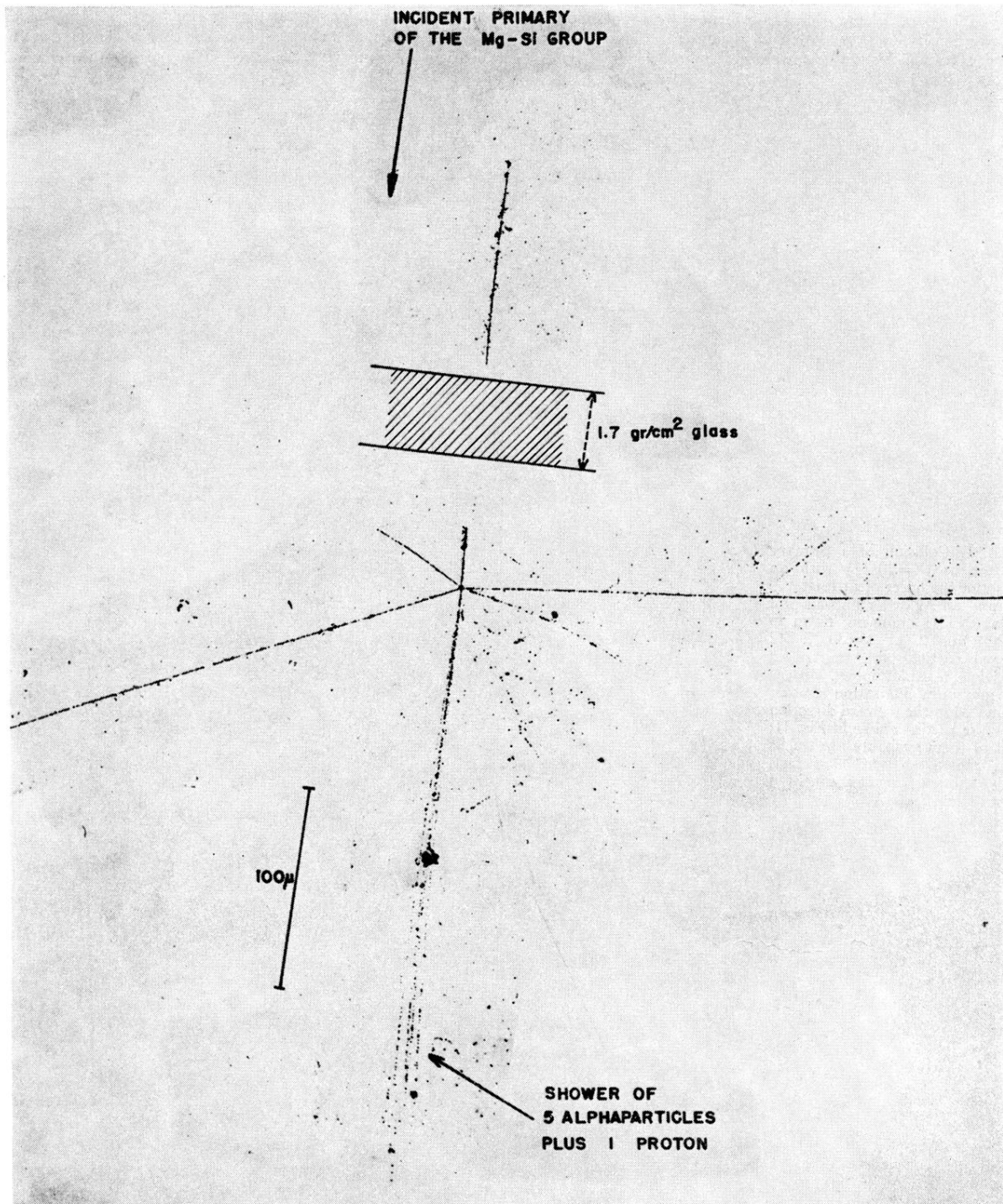


FIG. 2a. Collision of a nucleus of the Mg-Si group ( $Z \sim 12-14$ ), resulting in a narrow shower of five doubly charged relativistic particles ( $\alpha$ -particles) and one singly charged relativistic particle (proton). The particles of the shower, carrying 11 units of charge, are considered to be the products of the dissociation of the incident nucleus. A second minimum ionization track emerges with an angle of  $30^\circ$  with respect to the shower axis. Four low energy particles ejected from the star at large angles with respect to the direction of the primary are considered to be fragments of the target nucleus.

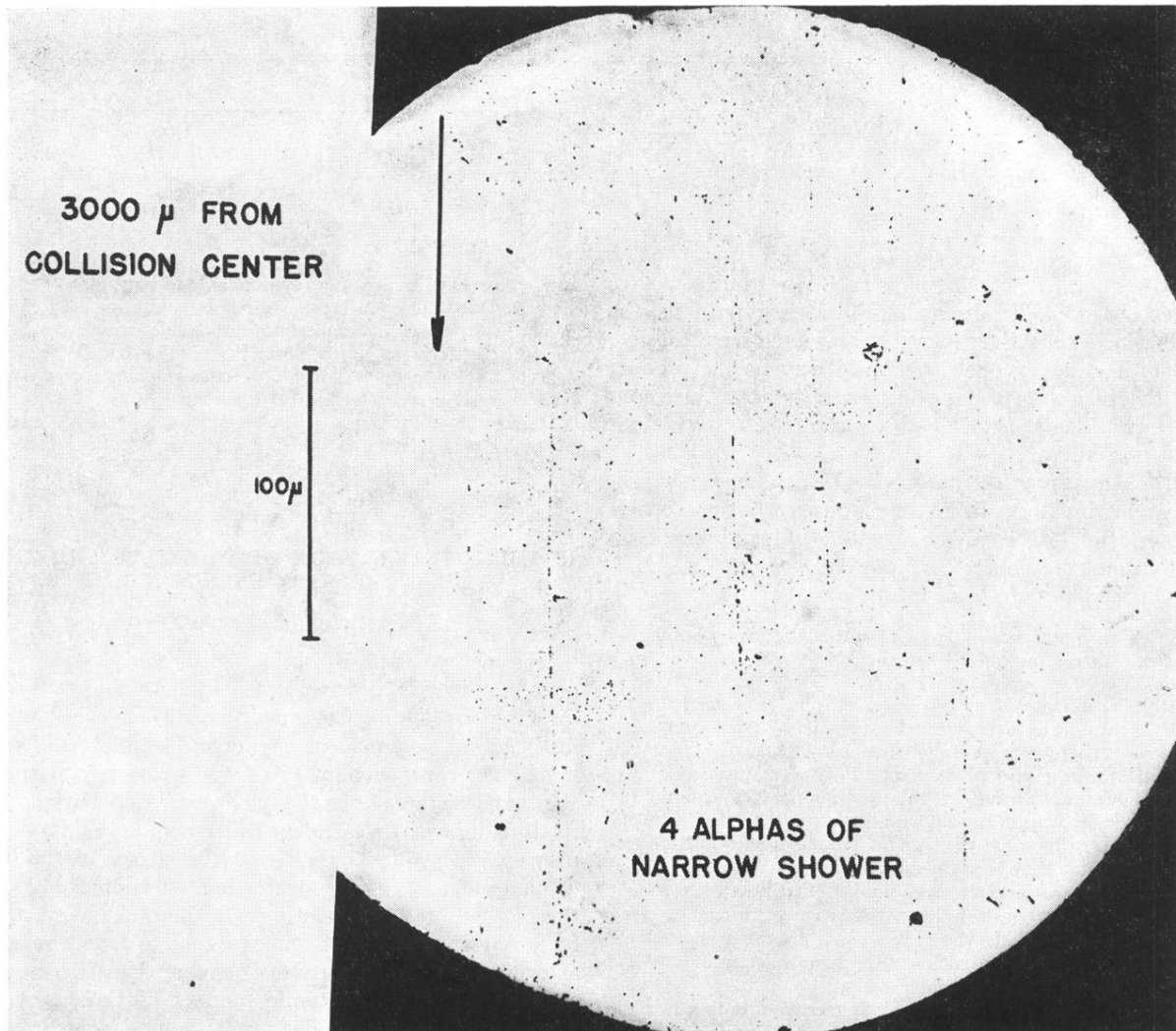


FIG. 2b. Tracks of 4 of the 5 alpha-particles of the shower of Fig. 2a as they appear in the next plate of the stack, after traversal of 3-mm glass. The average angle of the tracks of the five alpha-particles with respect to the axis of the shower is 0.03 radian, corresponding to an energy of the incident nucleus of  $\sim(3-4)$  Bev per nucleon.

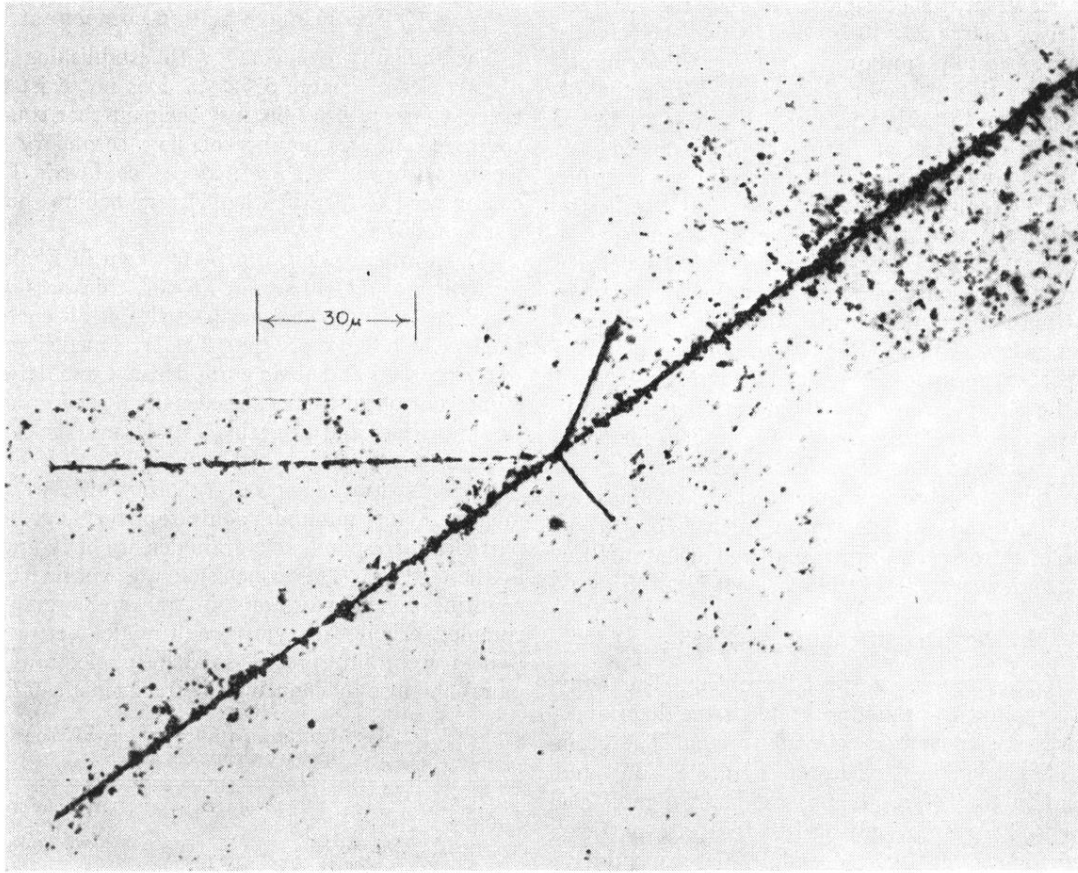


FIG. 5. A nucleus with charge  $Z \sim 20$  causes ejection of three charged particles from a target nucleus without suffering any noticeable deflection or loss of charge. This event, which was observed by Dr. E. O. Salant and Dr. J. Hornbostel, may be the result of a rather distant collision. (Courtesy of Dr. E. O. Salant and Dr. J. Hornbostel, Brookhaven National Laboratory.)